Cardiovascular Research Advance Access published June 5, 2010

Cardiovascular Research
doi:10.1093/cvr/cvq133

Up-regulation of type 2 iodothyronine deiodinase in dilated cardiomyopathy

Yuan-Yuan Wang[1], Sachio Morimoto[1]*, Cheng-Kun Du[1], Qun-Wei Lu[1,2], Dong-Yun Zhan[1], Takaki Tsutsumi[3], Tomomi Ide[3], Yosikazu Miwa[1], Fumi Takahashi-Yanaga[1], and Toshiyuki Sasaguri[1]

[1]Department of Clinical Pharmacology, Faculty of Medical Sciences, Kyushu University, 3-1-1 Maidashi, Higashi-ku, Fukuoka 812-8582, Japan; [2]Department of Physiology and Biophysics, Center for Cardiovascular Research, College of Medicine, University of Illinois at Chicago, Chicago, IL 60612, USA; and [3]Department of Cardiovascular Medicine, Faculty of Medical Sciences, Kyushu University, Fukuoka 812-8582, Japan

Received 9 November 2009; revised 2 May 2010; accepted 3 May 2010

Time for primary review: 41 days

Aims Thyroid hormone (TH) has prominent effects on the heart, and hyperthyroidism is occasionally found to be a cause of dilated cardiomyopathy (DCM). We aim to explore the potential role of TH in the pathogenesis of DCM.

Methods and results The pathophysiological role of TH in the heart was investigated using a knock-in mouse model of inherited DCM with a deletion mutation ΔK210 in the cardiac troponin T gene. Serum tri-iodothyronine (T_3) levels showed no significant difference between wild-type (WT) and DCM mice, whereas cardiac T_3 levels in DCM mice were significantly higher than those in WT mice. Type 2 iodothyronine deiodinase (Dio2), which produces T_3 from thyroxin, was up-regulated in the DCM mice hearts. The cAMP levels were increased in DCM mice hearts, suggesting that transcriptional up-regulation of Dio2 gene is mediated through the evolutionarily conserved cAMP-response element site in its promoter. Propylthiouracil (PTU), an anti-thyroid drug, prevented the hypertrophic remodelling of the heart in DCM mice and improved their cardiac function and life expectancy. Akt and p38 mitogen-activated protein kinase (p38 MAPK) phosphorylation increased in the DCM mice hearts and PTU treatment significantly reduced the phosphorylation levels, strongly suggesting that Dio2 up-regulation is involved in cardiac remodelling in DCM through activating the TH-signalling pathways involving Akt and p38 MAPK. Dio2 gene expression was also markedly up-regulated in the mice hearts developing similar eccentric hypertrophy after myocardial infarction.

Conclusion Local hyperthyroidism via transcriptional up-regulation of the *Dio2* gene may be an important underlying mechanism for the hypertrophic cardiac remodelling in DCM.

Keywords Dilated cardiomyopathy • Myocardial infarction • Hypertrophy • Thyroid hormone

1. Introduction

Changes in the serum level of the thyroid hormone (TH) affect various organs of the body, among which the heart is one of the most sensitive. Patients with hypothyroidism have decreased cardiac contractility and cardiac output.[1] On the other hand, patients with hyperthyroidism have increased cardiac contractility and cardiac output, with an increased left ventricular (LV) mass due to eccentric cardiac hypertrophy[2]; however, patients with severe, long-standing hyperthyroidism may occasionally have poor cardiac contractility, low cardiac output, and symptoms and signs of congestive heart failure associated with dilated cardiomyopathy (DCM).[3–10]

Recently, we developed a knock-in mouse model of DCM, in which deletion of 3 base pairs coding for K210 in cardiac troponin T (cTnT), found in familial DCM patients, was introduced into the endogenous mouse *Tnnt2* gene using embryonic stem cell technology.[11,12] The mutant mice developed marked eccentric cardiac hypertrophy with LV systolic dysfunction and frequent sudden death, closely recapitulating human phenotypes. The cardiac muscle of mutant mice showed significantly lower Ca^{2+} sensitivity of force generation and greater amplitude of Ca^{2+} transient than the wild-type (WT) mice, suggesting that mutant mice develop eccentric cardiac hypertrophy with augmented Ca^{2+} transient to compensate for reduced pump function.

* Corresponding author. Tel: +81 92 642 6081; fax: +81 92 642 6084, Email: morimoto@med.kyushu-u.ac.jp

In the present study, we sought to explore the potential involvement of hyperthyroidism or thyrotoxicosis in the pathogenesis of DCM by using this mouse model. Although there was no significant difference in serum tri-iodothyronine (T_3) levels between DCM and WT mice, we found that DCM mice have significantly higher T_3 levels in the heart than WT mice. Further analyses revealed that type 2 iodothyronine deiodinase (Dio2), which produces the active hormone T_3 by catalysing outer ring de-iodination of the pro-hormone thyroxin (T_4),[13] was transcriptionally up-regulated in the hearts of DCM mice. Transcriptional up-regulation of Dio2 occurred in the mice hearts developing similar eccentric hypertrophy after myocardial infarction (MI) (i.e. ischaemic DCM). The findings of the present study provide novel evidence that local cardiac hyperthyroidism, induced by Dio2 up-regulation, may play an important role in the hypertrophic remodelling of the heart in DCM, and that anti-thyroid drugs may be beneficial for the treatment of this heart disease.

2. Methods

2.1 Animal models

A knock-in mouse model, in which 3 base pairs coding for K210 in cTnT were deleted from the endogenous gene *Tnnt2*, was developed as described elsewhere.[11] Homozygous mutant mice were obtained by crossing heterozygous mutant mice, which had been backcrossed to the C57BL/6J line at least 10 generations. Mixed-gender 8-week-old homozygous mutant mice and WT mice from the same colony were used as DCM and non-DCM models, respectively. An MI model was developed using 8-week-old ICR mice by ligating the left anterior descending coronary artery (LAD) for 4 weeks according to the methods described by Michael *et al.*[14] The investigation conforms to the Guide for the Care and Use of Laboratory Animals published by the US National Institutes of Health (NIH Publication No. 85-23, revised 1996). The experimental protocol was reviewed by the Committee of Ethics on Animal Experiments of the Faculty of Medicine, Kyushu University, Japan. This study was performed according to the Guidelines for Animal Experiments of the Faculty of Medicine, Kyushu University, and The Law (No. 105) and Notification (No. 6) of the Japanese Government.

2.2 Determination of T_3 level

Serum and cardiac T_3 levels were determined using a solid-phase competitive enzyme immunoassay (EIA) kit (Free T3 Micro-ELISA Test Kit, Leinco Technologies). Serum T3 levels were determined following the manufacturer's instruction. T_3 level of the heart was determined as follows. Ventricles were homogenized in 5% trichloroacetic acid (TCA), a strong protein denaturant, using a polytron homogenizer, followed by centrifugation at 15 000 rpm for 10 min at 4°C. The precipitate was solubilized with 1 M NaOH, and the total amount of protein was determined by the Bradford method. The protein-free supernatant was assayed for T_3 after TCA was extracted twice using water-saturated ether.

2.3 Real-time quantitative reverse transcriptase–polymerase chain reaction

Total RNAs were extracted from tissues after homogenization in TRIzol (Invitrogen) using a polytron homogenizer. First-strand cDNAs were synthesized from 2 μg of total RNA using a high-capacity cDNA reverse transcription kit (Applied Biosystems). TaqMan quantitative polymerase chain reaction (PCR) reactions were then carried out in 50 μL mixtures containing 22.5 μL of first-strand cDNA diluted with RNase-free water, 25 μL of TaqMan Universal 2× PCR Master Mix (Applied Biosystems), and 2.5 μL of 20× TaqMan Gene Expression Assay [Mm0083935_m1, Dio1, Mm00515664-m1 Dio2, Mm00548953_s1 Dio3, Mm99999915_g1 glyceraldehyde 3-phosphate dehydrogenase (GAPDH)] with an ABI Prism 7500 (Applied Biosystems).

2.4 cDNA microarrays

Ventricles were homogenized in TRIzol (Invitrogen) using a polytron homogenizer. Total RNA was then isolated according to the manufacturer's instructions. RNA samples (500 ng) with A260/A280 and A260/A230 ratios >2 were amplified and labelled with Cy5- and Cy3-CTP using an Agilent Low RNA Input Fluorescent Linear Amplification Kit (Agilent Technologies). Labelled cRNA samples were then purified using RNeasy mini spin columns (QIAGEN). Cy5-labelled WT and Cy3-labelled mutant mouse samples (1 μg each) were mixed and incubated with an Agilent 22K 60-mer Mouse Oligo Microarray slide using an Agilent *In Situ* Hybridization Kit Plus (Agilent Technologies). After drying, the slides were scanned at 10 μm resolution using an Agilent Technologies Microarray Scanner (Agilent Technologies). The complete microarray data are available at the ArrayExpress database under accession no. E-MEXP-1340.

2.5 Determination of cAMP level

Hearts were excised from mice under anaesthesia with pentobarbital sodium [50 mg/kg, intraperitoneally (i.p.)]. After a brief perfusion of an isolated heart with oxygenated Krebs–Henseleit solution at 37°C in the Langendorff mode, ventricles were dissected from the hearts and immediately freeze-clamped by liquid N_2. The frozen tissues were mechanically crushed into powder and denatured in 6 vol. of 5% TCA by freezing (−80°C) and thawing three times. After centrifugation at 15 000 rpm for 10 min at 4°C, the total amount of protein in the precipitate solubilized by 1 M NaOH was determined by the Bradford method. The supernatant was assayed for cAMP using a Cyclic AMP EIA Kit (Cayman Chemical) after extracting the TCA twice using water-saturated ether.

2.6 Drug administration

6-Propyl-2-thiouracil (PTU) and (±)-metoprolol (+)-tartrate salt were purchased from Sigma-Aldrich (USA). Carvedilol was supplied by Nippon DIICHI SANKYO Co., Ltd (Japan). Atenolol was purchased from Wako Pure Chemical Industries, Ltd (Japan). Mice were injected i.p. with PTU (12 mg/kg) once daily for 4 weeks from 30 days of age, while being fed an iodine-free diet. Control mice were injected i.p. with vehicle only (physiological saline containing 15 mM NaOH), while being fed a normal diet. Metoprolol, carvedilol, and atenolol were suspended in 0.25% methylcellulose solution and administered orally to DCM mice (8-week-old) at a dose of 30, 10, and 10 mg/kg, respectively. At 2 h after administration, the hearts were excised and analysed for the protein expression level of Dio2.

2.7 Myosin isoform separation, histochemistry, and echocardiography

Quantification of myosin heavy chain (MyHC) isoforms, histochemistry, and echocardiography were performed as described previously.[11]

2.8 Western blot analysis

After a brief perfusion of the isolated heart with oxygenated Krebs–Henseleit solution at 37°C in a Langendorff mode to remove blood from the myocardium, ventricles were dissected from the heart, blotted on filter paper, and homogenized in Laemmli's sample buffer. LV homogenate samples were subjected to western blot analysis as described previously,[15] using an anti-cardiac ankyrin repeat protein (CARP) polyclonal antibody (sc-23253, Santa Cruz); an anti-Dio2 polyclonal antibody (ab77481, Abcam); an anti-TH receptor α_1 ($TR\alpha_1$) polyclonal antibody (PA1-211A, BioReagents); an anti-$TR\beta_1$ monoclonal antibody (MA1-216,

Affinity BioReagents); an anti-phospho-Akt (Ser473) polyclonal antibody (No. 9271, Cell Signaling Technology); an anti-phosph-p38 mitogen-activated protein kinase (MAPK) (Thr180/Tyr182) polyclonal antibody (No. 9211, Cell Signaling Technology); an anti-Akt polyclonal antibody (No. 9272, Cell Signaling Technology); an anti-p38 MAPK polyclonal antibody (No. 9212, Cell Signaling Technology); an anti-phospholamban (PLB) monoclonal antibody (ab2865, Abcam); an anti-sarcoplasmic/endoplasmic reticulum (ER) Ca^{2+}-ATPase 2a (SERCA2a) monoclonal antibody (ab2861; Abcam); an anti-GAPDH monoclonal antibody (ab9484, Abcam); and an anti-histone H3 monoclonal antibody (05-499, Upstate).

2.9 Isolation of cardiomyocytes and non-cardiomyocytes from the mouse heart

Cells were isolated from the LV myocardium as described previously.[11] Cardiomyocytes and non-cardiomyocytes were separated by the density centrifugation method with 40 and 60% Percoll. Aliquots of cardiomyocyte and non-cardiomyocyte suspensions were plated on laminin- and gelatin-coated culture dishes and then cultured in DMEM supplemented with and without 10% foetal bovine serum, respectively. To measure T_3 production by cells, media and cells were assayed for T_3 after 2 h incubation in the presence of 100 nM T_4. To examine the effect of forskolin on

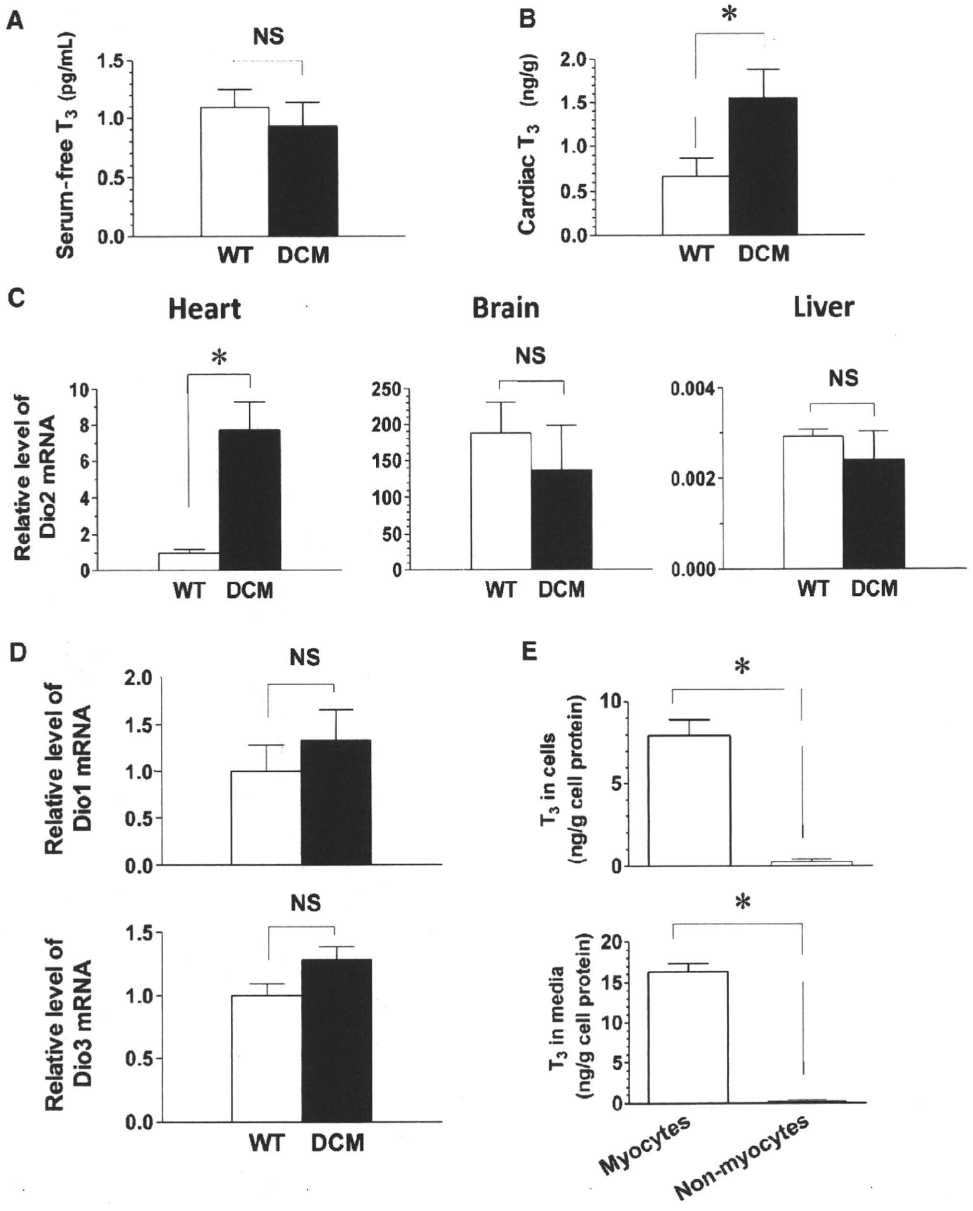

Figure 1 Increased T_3 levels and transcriptional up-regulation of Dio2 in the myocardium of DCM mice. (*A*) Serum-free T_3 levels. (*B*) T_3 levels in the heart, determined by using homogenates of the ventricle. (*C*) Dio2 mRNA expression levels in the heart, brain, and liver. (*D*) Expression levels of Dio1 and Dio3 mRNA in the heart. (*E*) T_3 production in isolated cardiomyocytes and non-cardiomyocytes from the DCM mouse heart. Findings in (A)–(D) show the results from data obtained from five mice (8-week-old), respectively. Findings in (E) represent the results from data obtained from three separate cell cultures. *$P < 0.05$. See Methods for experimental details.

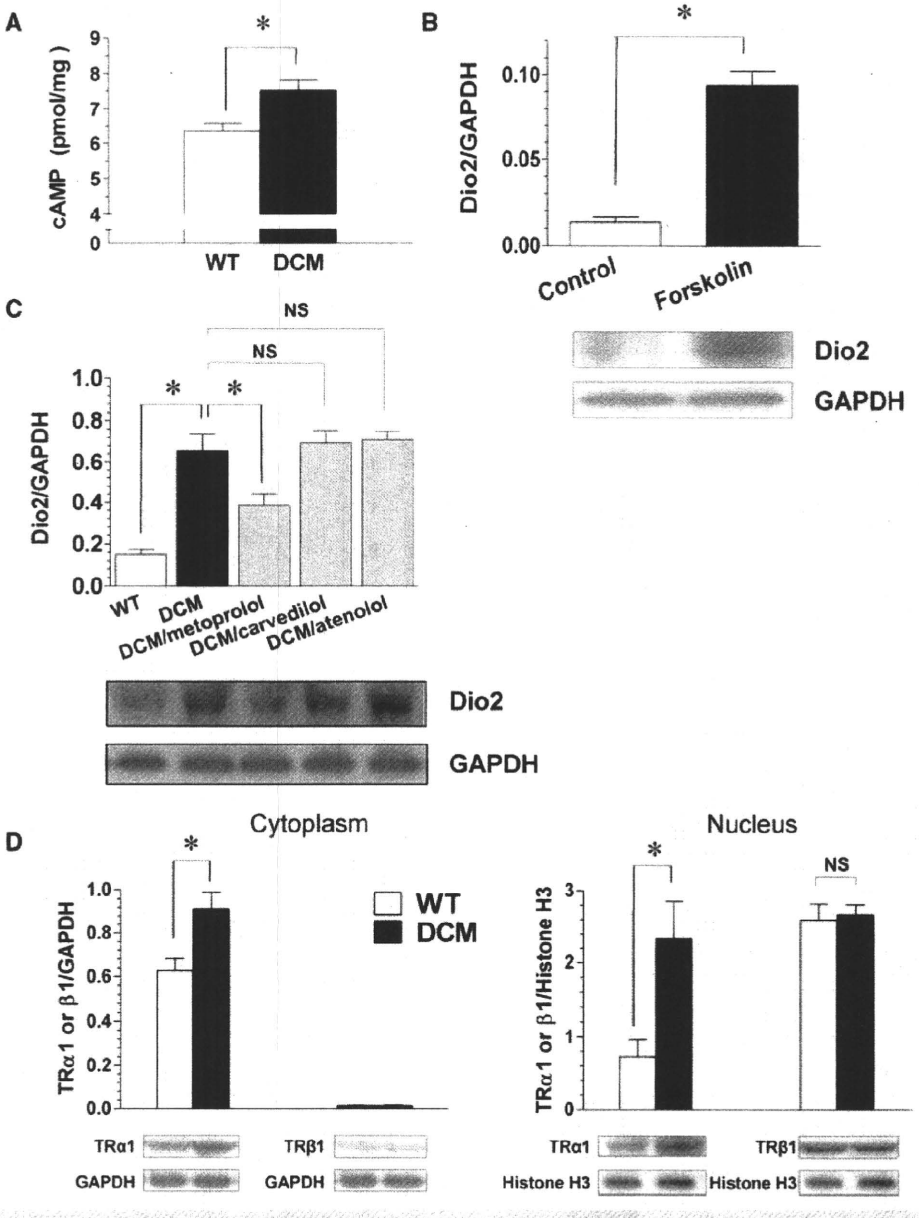

Figure 2 cAMP-mediated Dio2 expression in myocardium of DCM mice. (*A*) Intracellular cAMP levels in the heart. (*B*) Induction of Dio2 protein expression by forskolin in isolated cardiomyocytes from the WT mouse heart. (*C*) Effects of oral administration of β-blockers on Dio2 expression in the DCM mouse heart. (*D*) $TR\alpha_1/\beta_1$ expression levels in cytoplasmic and nuclear fractions prepared from homogenates of the ventricle. Subcellular fractionation was carried out as described previously.[11] Findings in (A) and (D) and those in (C) show the results from data obtained from five and seven mice (8-week-old), respectively. Findings in (B) represent the results from data obtained from three separate cell cultures. $^*P < 0.05$. See Methods for experimental details.

Dio2 expression, cardiomyocytes harvested after 2 h incubation in the presence of 10 μM forskolin were analysed for the protein expression level.

2.10 Statistical analysis

Data are presented as mean ± SEM. Mean values for more than three groups were compared by one- or two-way ANOVA, followed by a *post hoc* Tukey's test. The difference between two mean values was analysed with an unpaired Student's *t*-test. If the data did not conform to a normal distribution, log-transformation was performed before statistical analysis to create a normal distribution. Survival data utilized the standard Kaplan–Meier analysis. $P < 0.05$ was considered to be significant.

3. Results

3.1 Increased T_3 levels and transcriptional up-regulation of Dio2 in the myocardium of DCM mice

No significant difference was found in serum-free T_3 level between WT and DCM mice (*Figure 1A*). However, we found that DCM mice had a much higher T_3 level in the heart (*Figure 1B*). Intracellular levels of T_3 in extra-thyroidal tissues such as brain are thought to be

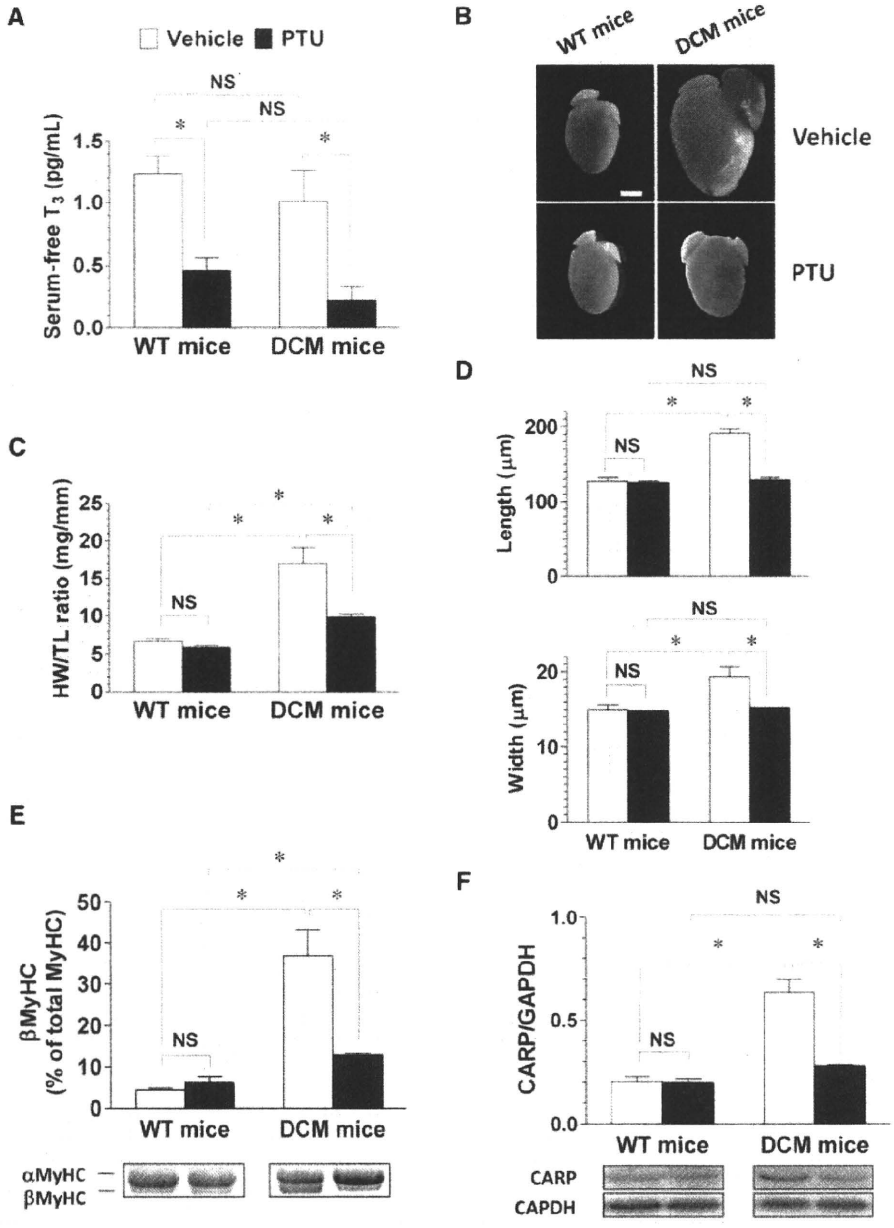

Figure 3 Effects of PTU treatment on hypertrophic remodelling of the heart in DCM mice. (*A*) Serum-free T_3 levels ($n = 3$ mice/group). (*B*) Gross morphology of the heart. Scale bar: 2 mm. (*C*) Heart weight to tibia length ratio (HW/TL) ($n = 10$–12 mice/group). (*D*) Size of cardiomyocytes ($n = 150$ cardiomyocytes isolated from three hearts/group). (*E*) Protein expression level of βMyHC in LV myocardium ($n = 3$ mice/group). (*F*) Protein expression level of CARP in LV myocardium ($n = 4$ mice/group).

regulated by changes in the activity of three isoenzymes of iodothyronine deiodinase (i.e. Dio1, Dio2, and Dio3) in an adaptive manner to compensate for environmental or internal changes.[16,17] Real-time quantitative reverse transcriptase (RT)–PCR analyses showed that the expression of Dio2 mRNA was organ-specifically up-regulated in the heart of DCM mice (*Figure 1C*), whereas the expression of Dio1 and Dio3 remained unchanged (*Figure 1D*). Dio2 is an ER-resident integral membrane protein that produces T_3 via the removal of an iodine moiety from T_4 in the cytoplasm.[13] Therefore, cardiac-specific up-regulation of Dio2 expression explains the local increase of T_3 levels in the heart of DCM mice. Cell culture experiments showed that cardiomyocytes, but not non-cardiomyocytes, produced significant amounts of T_3 from T_4 (*Figure 1E*), indicating that cardiomyocytes are the specific origin of T_3 production in the heart. The mammalian *Dio2* gene has an evolutionarily conserved cAMP-response element (CRE) site in the promoter, through which cAMP activates the transcription of the *Dio2* gene.[18] DCM mice had a significantly higher level of cAMP in the heart compared with WT mice (*Figure 2A*). Direct activation of adenylate cyclase by forskolin induced the expression of Dio2 protein in isolated cardiomyocytes (*Figure 2B*). Oral administration of metoprolol, a lipophilic β_1-selective β-adrenoceptor blocker, significantly

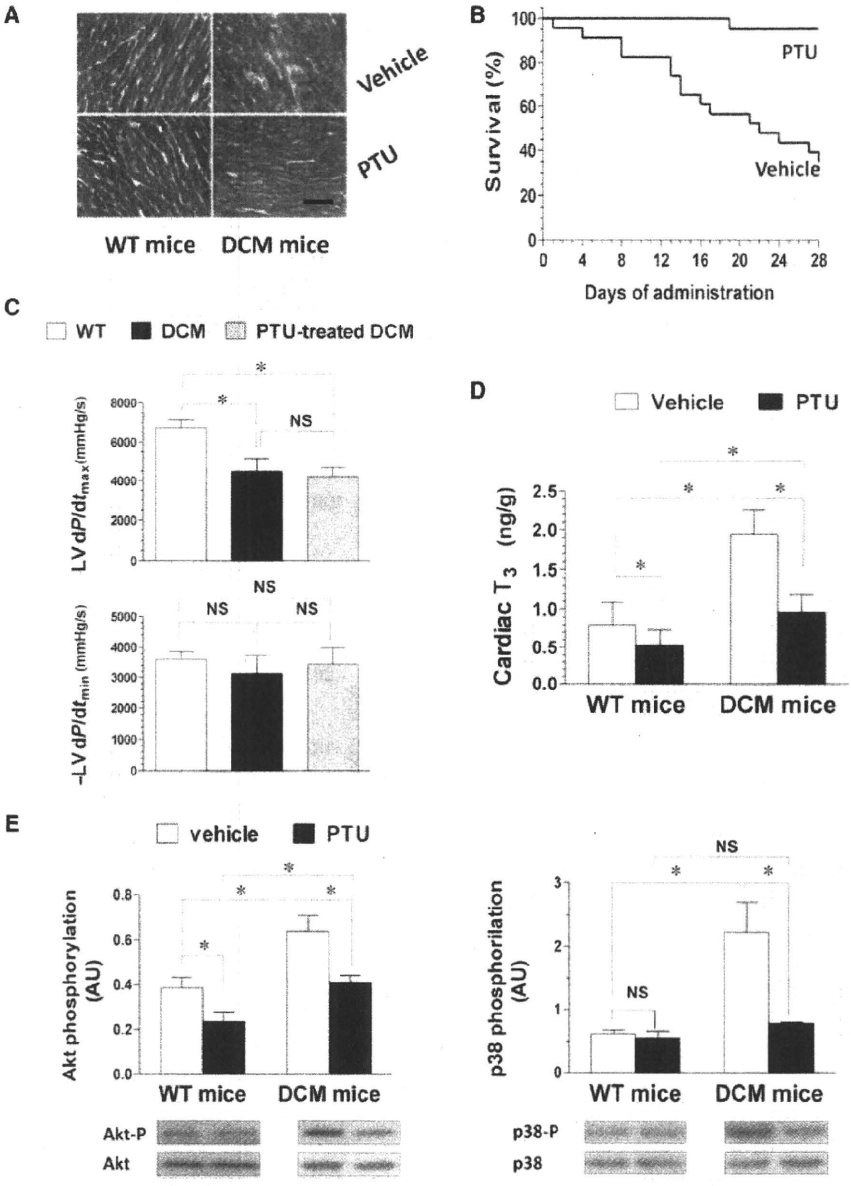

Figure 4 Effects of PTU treatment on disease progression in DCM mice. (*A*) Histology of left ventricles. Connective tissues were stained blue with azan. Scale bar: 100 μm. (*B*) Kaplan–Meier survival curves for DCM mice treated with vehicle only ($n = 23$) and PTU ($n = 21$). The log-rank test demonstrated significant differences between the two survival curves ($P < 0.0001$). (*C*) Maximum or minimum derivative of LV pressure ($n = 7$ mice/group). (*D*) T_3 levels in ventricles ($n = 3$ mice/group). (*E*) Phosphorylation levels of Akt and p38 MAPK in ventricles ($n = 3$ mice/group). *$P < 0.05$.

decreased the expression level of the Dio2 protein in DCM mice, whereas carvedilol, a lipophilic non-selective β-blocker, and atenolol, hydrophilic β_1-selective β-blocker, had no effects on the Dio2 expression level (*Figure 2C*). We have previously shown that tonic activation level of the efferent cardiac vagal nerves is significantly decreased in DCM mice and that metoprolol, but not carvedilol or atenolol, can prevent cardiac dysfunction and remodelling and extend the survival by activating the vagal nervous outflow to the heart, possibly due to an inhibition of β_1-adrenoceptor in the central nervous system.[15] These findings suggest that transcriptional up-regulation of Dio2 is mediated by chronic increases in the intracellular cAMP level, probably due to the inhibited vagal nervous outflow, as well as the activated sympathetic outflow, to the heart via baroreflex.

TH receptor α_1 ($TR\alpha_1$) protein expression was significantly up-regulated in both the cytoplasm and nucleus of DCM mouse cardiomyocytes, whereas $TR\beta_1$ protein expression remained unchanged (*Figure 2D*).

3.2 cDNA microarray analysis

cDNA microarray analysis of the hearts confirmed that Dio2 mRNA expression was significantly up-regulated in DCM mice

(Supplementary material online, *Figure S1A*). This analysis provided further information regarding genes that may be involved in the pathogenesis of DCM. The foetal gene programme [α-skeletal actin (SkA), atrial natriuretic peptide (ANP), brain natriuretic peptide (BNP), and βMyHC] was re-activated in the heart of DCM mice, indicating that cardiomyocytes underwent 'pathological' hypertrophic remodelling (Supplementary material online, *Figure S1B*). CARP, a genetic marker for cardiac hypertrophy involving p38 MAPK,[19] was also up-regulated in DCM mice (Supplementary material online, *Figure S1B*). The insulin-like growth factor 1 (IGF-1) and transforming growth factor β (TGFβ), known to act in an autocrine/paracrine manner during pathological hypertrophy,[20,21] were also up-regulated in DCM mice (Supplementary material online, *Figure S1C*).

3.3 Effects of anti-thyroid drug on disease progression in DCM mice

We examined the effects of PTU, an anti-thyroid drug, on disease progression in DCM mice. PTU treatment significantly decreased serum-free T_3 levels in WT and DCM mice to a similar level (*Figure 3A*). PTU treatment had profound effects on DCM mice in preventing cardiac enlargement (*Figure 3B* and *C*) and myocyte hypertrophy (*Figure 3D*), and decreased the expression of hypertrophic markers βMyHC and CARP (*Figure 3E* and *F*). On the other hand, PTU had no significant effects on WT mice cardiac gross morphology, myocyte size, and hypertrophic marker expression. PTU treatment increased the expression of PLB and decreased the expression of SERCA2a in both WT and DCM mice (Supplementary material online, *Figure S2*), consistent with the well-known behaviour of these proteins under hypothyroidic conditions.[22] PTU treatment also prevented myocardial fibrosis in DCM mice (*Figure 4A*) and significantly improved lifespan (*Figure 4B*). PTU treatment significantly increased the ejection fraction (EF) of the DCM mouse heart in a dose-dependent manner (*Table 1*). However, PTU treatment did not significantly restore the maximum rate of LV pressure change (*Figure 4C*), suggesting that a reduction in circumferential stress due to decreased LV end-diastolic diameter through anti-hypertrophic effect of PTU may, at least in part, contribute to the moderately increased EF after long-term PTU treatment (*Table 1*). Cardiac T_3 in DCM mice was reduced to a level similar to that of WT mice after PTU treatment (*Figure 4D*). These results strongly suggest that local activation of T_3 production by transcriptional up-regulation of the *Dio2* gene in the heart plays an important role in the formation of eccentric cardiac hypertrophy and myocardial degeneration in DCM mice.

Recently, two distinct non-nuclear TH-signalling pathways—$TR\alpha_1$-phosphatidylinositol 3-kinase (PI3K)-Akt-mammalian target of rapamycin (mTOR)-S6 kinase 1 (S6K1) and $TR\alpha_1$-TGFβ-activated kinase 1 (TAK1)-p38 MAPK—have been shown to be involved in physiological and pathological cardiac hypertrophy, respectively.[23,24] Phosphorylation levels of Akt and p38 MAPK were significantly higher in the hearts of DCM mice in comparison with WT mice, and PTU treatment significantly decreased the higher phosphorylation levels of Akt and p38 MAPK (*Figure 4E*), suggesting that these two non-nuclear TH-signalling pathways are involved in hypertrophic remodelling of DCM mice hearts.

3.4 Dio2 expression in post-MI mice

To determine whether transcriptional up-regulation of Dio2 is a general phenomenon in DCM, we developed a mouse model of post-MI by coronary artery ligation, known to cause a similar DCM phenotype with eccentric cardiac hypertrophy. Post-MI mice developed markedly enlarged hearts with LV systolic dysfunction (*Figure 5A* and *Table 2*), and Dio2 mRNA expression was found to be markedly up-regulated in the heart (*Figure 5B*). PTU treatment prevented hypertrophic remodelling of hearts in post-MI mice (*Table 2*). These results strongly suggest that local hyperthyroidism via Dio2 up-regulation in the heart is also involved in eccentric cardiac hypertrophy after MI.

4. Discussion

TH has a cardiac growth-promoting effect,[3,25] in which serum-free T_4 and T_3 enter the cell via TH transporters.[26] In cardiomyocytes,

Table 1 Echocardiography data of DCM mice receiving vehicle or PTU treatment

	WT mice		DCM mice		
	Vehicle	PTU (12 mg/kg)	Vehicle	PTU (4 mg/kg)	PTU (12 mg/kg)
Mice (*n*)	12	10	11	6	10
Age (weeks)	8	8	8	8	8
BW (g)	22.4 ± 0.8	19.8 ± 0.7	20.4 ± 1.1	19.1.4 ± 0.9	18.6 ± 1.1*
HR (bpm)	369 ± 9	369 ± 6	379 ± 6	399 ± 7	385 ± 4
IVST (mm)	0.50 ± 0.02	0.47 ± 0.02	0.55 ± 0.03*	0.45 ± 0.02**	0.43 ± 0.02**
LVPWT (mm)	0.53 ± 0.03	0.47 ± 0.03	0.51 ± 0.02	0.43 ± 0.02	0.38 ± 0.02*, ***
LVESD (mm)	2.42 ± 0.09	2.49 ± 0.06	4.80 ± 0.18*****	4.43 ± 0.30*****	4.02 ± 0.11******
LVEDD (mm)	3.60 ± 0.07	3.63 ± 0.08	5.61 ± 0.17*****	5.33 ± 0.26*****	4.91 ± 0.12******
EF (%)	68.4 ± 2.1	65.2 ± 1.1	34.0 ± 1.4*****	41.0 ± 3.2*****	42.9 ± 0.8******

PTU or vehicle was i.p. administered to WT and DCM mice once daily for 4 weeks from 30 days of age. Statistical significance was determined by one-way analysis of variance followed by the *post hoc* Tukey's multiple comparison test.

BW, body weight; HR, heart rate; bpm, beats per minute; IVST, interventricular septal wall thickness; LVPWT, LV posterior wall thickness; LV, left ventricular; LVESD, LV end-systolic dimension; LVEDD, LV end-diastolic dimension; EF, ejection fraction.

*$P < 0.05$ vs. PTU (12 mg/kg)-treated WT mice.

**$P < 0.05$ vs. vehicle-treated DCM mice.

***$P < 0.05$ vs. vehicle-WT mice.

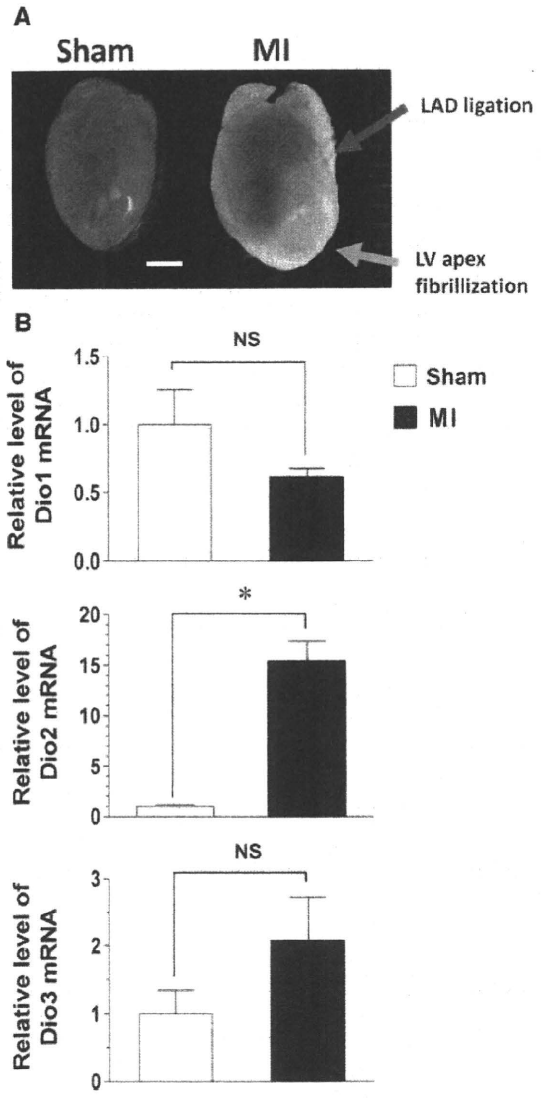

Figure 5 Dio expression in post-MI mice. (*A*) Gross morphology of the hearts of sham-operated and MI mice. LAD, left anterior descending coronary artery; LV, left ventricle; MI, myocardial infarction. Scale bar: 2 mm. (*B*) Dio1, Dio2, and Dio3 mRNA expression levels in ventricles of sham-operated and MI mice as determined by TaqMan quantitative real-time RT–PCR ($n = 5$ mice/group). *$P < 0.05$.

Table 2 Echocardiography data of MI mice

	Sham-operated mice	MI mice	PTU-treated MI mice
Mice (*n*)	6	7	8
Age (weeks)	12	12	12
HW (mg)	194.4 ± 2.5	279.6 ± 9.1*	204.1 ± 6.8**
BW (g)	39.1 ± 0.3	35.9 ± 1.0*	35.9 ± 0.9*
HW/BW (mg/g)	4.97 ± 0.06	7.80 ± 0.23*	5.71 ± 0.26**
HR (bpm)	384 ± 9	372 ± 14	385 ± 16
IVST (mm)	0.52 ± 0.02	0.36 ± 0.02	0.50 ± 0.07
LVPWT (mm)	0.47 ± 0.02	0.46 ± 0.03	0.48 ± 0.06
LVESD (mm)	2.15 ± 0.12	5.49 ± 0.19*	5.17 ± 0.32*
LVEDD (mm)	3.55 ± 0.09	6.37 ± 0.21*	6.13 ± 0.24*
EF (%)	76.2 ± 2.3	33.1 ± 1.1*	38.9 ± 4.7*

PTU (12 mg/kg) was administered to MI mice i.p. once daily for 4 weeks just after ligating LAD. Statistical significance was determined by one-way analysis of variance followed by the *post hoc* Tukey's multiple comparison test.
HW, heart weight; MI, myocardial infarction.
*$P < 0.05$ vs. sham-operated mice.
**$P < 0.05$ vs. MI mice.

entered T_3 modulates the transcriptional activity of target genes through binding to nucleus-localized TR. However, this nuclear TH-signalling pathway cannot fully explain the cardiac growth-promoting effects of extracellular T_3.[3,25] Recent studies have demonstrated the presence of non-nuclear TH-signalling pathways, through which T_3 induces physiological or pathological cardiac growth by activating PI3K or TAK1 in the cytosol (*Figure 6*).[23,24] Kenessey and Ojamaa[27] and Kenessey *et al.*[28] have shown that TRα_1 localizes to both the nucleus and cytosol in cardiomyocytes. They subsequently demonstrated that cytosol-localized TRα_1 (like the oestrogen receptor ERα)[29] interacts directly with the p85α regulatory subunit of PI3K, and also that T_3 treatment of cardiomyocytes increases TRα_1-associated PI3K activity, resulting in the activation of the Akt-mTOR-S6K1-signalling pathway leading to physiological cardiac hypertrophy.[23] On the other hand, Kinugawa *et al.*[24] demonstrated another non-nuclear TH-signalling pathway in which T_3 activates cytosolic TRα_1-associated TAK1, resulting in the activation of the p38 MAPK-signalling pathway leading to pathological cardiac hypertrophy (associated with the re-activation of the foetal gene programme including SkA, ANP, BNP, and βMyHC).

The above mentioned two non-nuclear TH-signalling pathways in cardiomyocytes could explain the paradoxical growth-promoting effects of T_3 on the heart of patients with hyperthyroidism, leading to eccentric but compensated cardiac hypertrophy with enhanced pump function, which occasionally degenerates into DCM with systolic dysfunction.[2–10] Results of the present study provide strong evidence that TH is also involved in the pathogenesis of DCM through the local activation of the heart. Locally increased T_3 in the heart by transcriptional up-regulation of the *Dio2* gene would have a paradoxical growth-promoting effect on the heart via two non-nuclear TH-signalling pathways involving Akt and p38 MAPK, as with patients with hyperthyroidism. Our DCM mouse model had a decreased LVEF with significant myocardial fibrosis, suggesting that the heart undergoes some pathological remodelling. However, the DCM mice exhibited no overt symptoms of heart failure, such as decreased spontaneous movement activity and dyspnoea.[11] These findings suggest that physiological compensatory hypertrophy and pathological degenerative hypertrophy may coexist in the hearts of these DCM mice, consistent with findings that phosphorylation levels of Akt and p38 MAPK are both significantly elevated in hearts.

The hearts of DCM mice used in this study are thought to undergo structural remodelling to compensate for reduced myocardial contractility due to decreased myofilament Ca^{2+} sensitivity, resulting in progressive eccentric cardiac hypertrophy.[11] On the other hand, the hearts of post-MI mice are thought to undergo structural remodelling to compensate for reduced myocardial contractility due to cardiomyocyte death, resulting in progressive eccentric

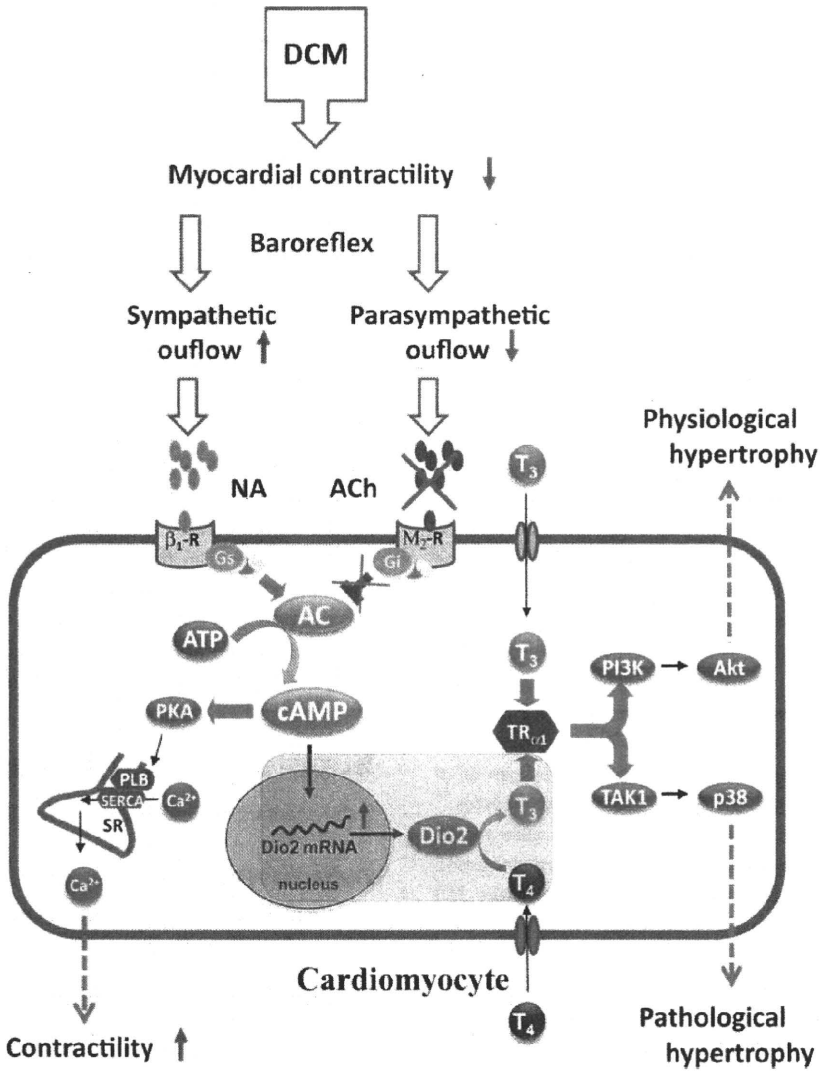

Figure 6 Molecular mechanism underlying eccentric cardiac hypertrophy in DCM and MI. 'Local hyperthyroidism in cardiomyocytes via Dio2 up-regulation', found in the present study (indicated in a semi-transparent box), links the well-known increase in cytosolic cAMP level due to activated sympathetic outflow to the heart via baroreflex in heart failure to the two, recently discovered, distinct 'non-nuclear TH-signalling pathways involving Akt and p38 MAPK', which lead to physiological and pathological cardiac hypertrophy, respectively. MI, myocardial infarction; NA, norepinephline; β_1-R, β_1-adrenergic receptor; Gs, stimulatory G protein; ACh, acetylcholine; M_2-R, M_2-muscarinic receptor; Gi, inhibitory G protein; AC, adenylate cyclase; PKA, protein kinase A; PLB, phospholamban; SERCA, sarcoplasmic/endoplasmic Ca^{2+}-ATPase; SR, sarcoplasmic reticulum; Dio2, type 2 iodothyronine deiodinase; T_4, thyroxine; T_3, tri-iodothyronine; TRα_1, thyroid hormone receptor α1; PI3K, phosphatidylinositol 3-kinase; Akt, protein kinase B; TAK1, transforming growth factor β-activated kinase 1; p38, p38 mitogen-activated protein kinase.

hypertrophy. Cardiomyocytes in these mice showed similar hypertrophic remodelling, characterized by myocyte elongation expected to lead to eccentric cardiac hypertrophy.[30] These facts raise an interesting hypothesis: local hyperthyroidism via Dio2 up-regulation in cardiomyocytes is generally involved in eccentric hypertrophy of the heart, stimulated by volume overload due to reduced myocardial contractility. Reduced myocardial contractility would be expected to activate sympathetic outflow and inhibit parasympathetic outflow to the heart via baroreflex, leading to chronic activation of adenylate cyclase via the stimulation of β_1-adreneric receptor and M_2-muscarinic receptor in cardiomyocytes. The resultant persistent increase in intracellular cAMP level is expected to augment the intracellular Ca^{2+} transient as demonstrated in the previous study,[11] and also activate the transcription of the *Dio2* gene as demonstrated in the present study (*Figure 2B*) via the CRE site in its promoter (*Figure 6*).[18] The present study, together with the previous study,[15] indicates that the lipophilic β_1-selective β-blocker metoprolol prevents cardiac remodelling in DCM mice by effectively suppressing the cAMP-mediated Dio2 up-regulation probably through the vagal activation via the central nervous system as well as direct β_1-adreneric receptor blockade in the heart. However, further studies should be required to clarify whether other unknown pharmacological properties may explain the effectiveness of metoprolol.

The present study showed that TRα_1 protein expression was also up-regulated in both the cytoplasm and nucleus of the DCM mouse, consistent with the finding that TRα_1 protein expression is markedly increased in patients with DCM.[31] Interestingly, TRα_1 expression in the heart has been shown to be up-regulated by α_1-adrenergic receptor stimulation,[32] probably through the activation of protein kinase Cα.[28] Activation of sympathetic outflow to the heart via baroreflex might thus effectively cause local hyperthyroidism through the up-regulation of Dio2 and TRα_1 in cardiomyocytes of the DCM mouse model.

Trivieri *et al.*[33] reported that long-term Dio2 overexpression in the heart of transgenic mice prevented heart failure caused by experimental LV pressure overload for 9 weeks, which appears to be inconsistent with the results of our present study. However, it should be noted that pressure overload usually leads to concentric cardiac hypertrophy, in which TH might play totally different roles from those in eccentric cardiac hypertrophy developed in our DCM mouse model. In fact, Trivieri *et al.* reported that protection against heart failure due to LV pressure overload might be related to the reversal of local cardiac hypothyroidism, which they expected to be caused by a nearly five-fold increase in the expression of Dio3 [an enzyme that converts T_4 and T_3 into inactive metabolites, reverse-T_3 (rT_3) and 3,3′-T_2, respectively] in response to pressure overload for 9 weeks.[33] Simonides *et al.*[34] also reported increased expression of Dio3 and reduction in local T_3 content in concentric cardiac hypertrophy developed in a rat model of heart failure due to RV pressure overload. They suggested that up-regulation of Dio3 could be stimulated by hypoxia, which might be caused by decreased oxygen diffusion due to the markedly increased diameter of cardiomyocytes.[34] In contrast to these pressure overload models, our mouse model developed eccentric cardiac hypertrophy due to marked elongation of cardiomyocytes with a marginal increase in diameter (*Figure 3D*) and caused no significant change in the Dio3 expression level (*Figure 1D*). It should also be noted that our mouse model of MI was developed by ligation of LAD for 4 weeks and thus most surviving cardiomyocytes undergoing hypertrophic remodelling must be no longer under hypoxic ischaemic conditions. Recently, Forini *et al.*[35] reported that T_3 administration to rat for 4 weeks from 3 days after MI halved infarct scar size and prevented the progression towards heart failure. These findings indicate that in some species and/or models, the T3 situation may differ from what we have reported here and that more data in other species and myocardial injury models will be required to generalize the role of Dio2 up-regulation in cardiac remodelling.

Hamilton *et al.*[36] showed that patients with congestive heart failure have a low serum T_3 level, which is the strongest predictor of short-term outcome. Iervasi *et al.*[37] also demonstrated that the low serum T_3 state is a strong predictor of death in a group of patients with heart disease with various aetiologies. Although these clinical studies showed a correlation between low serum T_3 level and poor prognosis in patients with heart disease, they did not demonstrate any causality. A decline in the serum T_3 level may be part of a host's mechanism of beneficial adaptation, known to occur in virtually all illnesses and patients undergoing major surgical procedures.[38] This could explain why no investigation has clearly demonstrated any beneficial effects of administering T_3 on mortality.[3] The DCM mice used in the present study showed no overt heart failure symptoms[11] and no significant decrease in serum T_3 level (*Figure 1A*). Nevertheless, they had a very high mortality rate due to ventricular fibrillation. This seems analogous to an observation of human heart failure patients, in which risk of sudden death increases with decreasing severity of heart failure.[39] PTU treatment dramatically prevented eccentric cardiac hypertrophy and extended the survival of DCM mice. These results suggest that lowering the serum TH level by anti-thyroid drug might be effective in preventing sudden death and progression of heart failure in DCM before the serum T_3 level begins to decrease through the host's adaptive mechanisms.

In summary, the results of the present study provide a novel molecular mechanism underlying eccentric cardiac hypertrophy and myocardial degeneration in DCM, in which locally increased T_3 in the heart by transcriptional up-regulation of Dio2 causes physiological and pathological cardiac hypertrophy through activating two distinct non-nuclear TH-signalling pathways, TRα_1-PI3K-Akt-mTOR-S6K1 and TRα_1-TAK1-p38 MAPK, respectively (*Figure 6*). However, the pathogenic role of transcriptional up-regulation of Dio2 remains rather speculative at present, and the relevance of the mechanism proposed in *Figure 6* should be tested by further experiments such as cardiac-specific knockdown or knockout of Dio2 in future research. Dio2 mRNA is expressed in the human heart about three times as much as in the rodent heart,[40] suggesting that Dio2 may play a more critical role in humans. Future studies are clearly required to explore whether local cardiac hyperthyroidism via Dio2 up-regulation also has a role in human heart diseases, and to validate the therapeutic implications of the findings of the present study.

Supplementary material

Supplementary material is available at *Cardiovascular Research* online.

Acknowledgements

We would like to thank Professor Iwao Ohtsuki at Jikei University School of Medicine for his valuable advice and encouragement.

Conflict of interest: none declared.

Funding

This work was supported by Special Coordination Funds from the Ministry of Education, Culture, Sports, Science, and Technology of Japan; Grants-in-Aid for Science Research (17300129) from the Japan Society for the Promotion of Science (JSPS); and grants from the Vehicle Racing Commemorative Foundation, the Mitsubishi Pharma Research Foundation, and the Institute of Seizon and Life Sciences to S.M. C.-K.D. is a recipient of the JSPS Postdoctoral Fellowship for Foreign Researchers.

References

1. Klein I, Danzi S. Thyroid disease and the heart. *Circulation* 2007;**116**:1725–1735.
2. Marcisz C, Jonderko G, Wroblewski T, Kurzawska G, Mazur F. Left ventricular mass in patients with hyperthyroidism. *Med Sci Monit* 2006;**12**:CR481–CR486.
3. Klein I, Ojamaa K. Thyroid hormone and the cardiovascular system. *N Engl J Med* 2001;**344**:501–509.
4. Safirstein SM, Santana O, Agatston AS. Thyrotoxicosis associated with reversible dilated cardiomyopathy. *Am Heart J* 1994;**128**:616–617.
5. Bauerlein EJ, Chakko CS, Kessler KM. Reversible dilated cardiomyopathy due to thyrotoxicosis. *Am J Cardiol* 1992;**70**:132.
6. Dhadke SV, Dhadke VN. Reversible cardiomyopathy. *J Assoc Physicians India* 2006;**54**: 740–741.
7. Londhey VA, Kamble US, Limaye CS, Pednekar SJ, Kini SH, Borges NE. Irreversible dilated cardiomyopathy due to thyrotoxicosis. *J Assoc Physicians India* 2006;**54**: 575–576.
8. Watanabe E, Ohsawa H, Noike H, Okamoto K, Tokuyama A, Kanai M *et al.* Dilated cardiomyopathy associated with hyperthyroidism. *Intern Med* 1995;**34**:762–767.
9. Kahaly GJ, Dillmann WH. Thyroid hormone action in the heart. *Endocr Rev* 2005;**26**: 704–728.

10. Osman F, Franklyn JA, Holder RL, Sheppard MC, Gammage MD. Cardiovascular manifestations of hyperthyroidism before and after antithyroid therapy: a matched case–control study. *J Am Coll Cardiol* 2007;**49**:71–81.
11. Du CK, Morimoto S, Nishii K, Minakami R, Ohta M, Tadano N *et al.* Knock-in mouse model of dilated cardiomyopathy caused by troponin mutation. *Circ Res* 2007;**101**: 185–194.
12. Morimoto S. Sarcomeric proteins and inherited cardiomyopathies. *Cardiovasc Res* 2008;**77**:659–666.
13. Baqui MM, Gereben B, Harney JW, Larsen PR, Bianco AC. Distinct subcellular localization of transiently expressed types 1 and 2 iodothyronine deiodinases as determined by immunofluorescence confocal microscopy. *Endocrinology* 2000;**141**: 4309–4312.
14. Michael LH, Entman ML, Hartley CJ, Youker KA, Zhu J, Hall SR *et al.* Myocardial ischemia and reperfusion: a murine model. *Am J Physiol* 1995;**269**:H2147–H2154.
15. Zhan DY, Morimoto S, Du CK, Wang YY, Lu QW, Tanaka A *et al.* Therapeutic effect of β-adrenoceptor blockers using a mouse model of dilated cardiomyopathy with a troponin mutation. *Cardiovasc Res* 2009;**84**:64–71.
16. Bianco AC, Kim BW. Deiodinases: implications of the local control of thyroid hormone action. *J Clin Invest* 2006;**116**:2571–2579.
17. Kohrle J. Local activation and inactivation of thyroid hormones: the deiodinase family. *Mol Cell Endocrinol* 1999;**151**:103–119.
18. Gereben B, Salvatore D. Pretranslational regulation of type 2 deiodinase. *Thyroid* 2005; **15**:855–864.
19. Aihara Y, Kurabayashi M, Saito Y, Ohyama Y, Tanaka T, Takeda S *et al.* Cardiac ankyrin repeat protein is a novel marker of cardiac hypertrophy: role of M-CAT element within the promoter. *Hypertension* 2000;**36**:48–53.
20. Donohue T, Dworkin L, Lango M, Fliegner K, Lango R, Benstein J *et al.* Induction of myocardial insulin-like growth factor-I gene expression in left ventricular hypertrophy. *Circulation* 1994;**89**:799–809.
21. Brand T, Schneider MD. The TGF beta superfamily in myocardium: ligands, receptors, transduction, and function. *J Mol Cell Cardiol* 1995;**27**:5–18.
22. Kiss E, Jakab G, Kranias EG, Edes I. Thyroid hormone-induced alterations in phospholamban protein expression. Regulatory effects on sarcoplasmic reticulum Ca^{2+} transport and myocardial relaxation. *Circ Res* 1994;**75**:245–251.
23. Kenessey A, Ojamaa K. Thyroid hormone stimulates protein synthesis in the cardiomyocyte by activating the Akt-mTOR and p70S6K pathways. *J Biol Chem* 2006;**281**: 20666–20672.
24. Kinugawa K, Jeong MY, Bristow MR, Long CS. Thyroid hormone induces cardiac myocyte hypertrophy in a thyroid hormone receptor alpha1-specific manner that requires TAK1 and p38 mitogen-activated protein kinase. *Mol Endocrinol* 2005;**19**: 1618–1628.
25. Dillmann WH. Cellular action of thyroid hormone on the heart. *Thyroid* 2002;**12**: 447–452.
26. Jansen J, Friesema EC, Milici C, Visser TJ. Thyroid hormone transporters in health and disease. *Thyroid* 2005;**15**:757–768.
27. Kenessey A, Ojamaa K. Ligand-mediated decrease of thyroid hormone receptor-alpha1 in cardiomyocytes by proteosome-dependent degradation and altered mRNA stability. *Am J Physiol Heart Circ Physiol* 2005;**288**:H813–H821.
28. Kenessey A, Sullivan EA, Ojamaa K. Nuclear localization of protein kinase C-alpha induces thyroid hormone receptor-alpha1 expression in the cardiomyocyte. *Am J Physiol Heart Circ Physiol* 2006;**290**:H381–H389.
29. Simoncini T, Hafezi-Moghadam A, Brazil DP, Ley K, Chin WW, Liao JK. Interaction of oestrogen receptor with the regulatory subunit of phosphatidylinositol-3-OH kinase. *Nature* 2000;**407**:538–541.
30. Prahash AJC, Gupta S, Anand IS. Myocyte response to β-adrenergic stimulation is preserved in the noninfarcted myocardium of globally dysfunctional rat hearts after myocardial infarction. *Circulation* 2000;**102**:1840–1846.
31. d'Amati G, di Gioia CR, Mentuccia D, Pistilli D, Proietti-Pannunzi L, Miraldi F *et al.* Increased expression of thyroid hormone receptor isoforms in end-stage human congestive heart failure. *J Clin Endocrinol Metab* 2001;**86**:2080–2084.
32. Pantos C, Mourouzis I, Xinaris C, Kokkinos AD, Markakis K, Dimopoulos A *et al.* Time-dependent changes in the expression of thyroid hormone receptor alpha 1 in the myocardium after acute myocardial infarction: possible implications in cardiac remodelling. *Eur J Endocrinol* 2007;**156**:415–424.
33. Trivieri MG, Oudit GY, Sah R, Kerfant BG, Sun H, Gramolini AO *et al.* Cardiac-specific elevations in thyroid hormone enhance contractility and prevent pressure overload-induced cardiac dysfunction. *Proc Natl Acad Sci USA* 2006;**103**:6043–6048.
34. Simonides WS, Mulcahey MA, Redout EM, Muller A, Zuidwijk MJ, Visser TJ *et al.* Hypoxia-inducible factor induces local thyroid hormone inactivation during hypoxic-ischemic disease in rats. *J Clin Invest* 2008;**118**:975–983.
35. Forini F, Lionetti V, Ardehali H, Pucci A, Cecchetti F, Ghanefar M *et al.* Early long-term L-T3 replacement rescues mitochondria and prevents ischemic cardiac remodeling in rats. *J Cell Mol Med* 2010; doi:10.1111/j.1582-4934.2010.01014.x. Published online ahead of print 20 January 2010.
36. Hamilton MA, Stevenson LW, Luu M, Walden JA. Altered thyroid hormone metabolism in advanced heart failure. *J Am Coll Cardiol* 1990;**16**:91–95.
37. Iervasi G, Pingitore A, Landi P, Raciti M, Ripoli A, Scarlattini M *et al.* Low-T3 syndrome: a strong prognostic predictor of death in patients with heart disease. *Circulation* 2003;**107**:708–713.
38. Utiger RD. Altered thyroid function in nonthyroidal illness and surgery. To treat or not to treat? *N Engl J Med* 1995;**333**:1562–1563.
39. MERIT-HF Study Group. Effect of metoprolol CR/XL in chronic heart failure: metoprolol CR/XL randomised intervention trial in congestive heart failure (MERIT-HF). *Lancet* 1999;**353**:2001–2007.
40. Dentice M, Morisco C, Vitale M, Rossi G, Fenzi G, Salvatore D. The different cardiac expression of the type 2 iodothyronine deiodinase gene between human and rat is related to the differential response of the dio2 genes to Nkx-2.5 and GATA-4 transcription factors. *Mol Endocrinol* 2003;**17**:1508–1521.
41. Mizukami Y, Yoshioka K, Morimoto S, Yoshida K. A novel mechanism of JNK1 activation. Nuclear translocation and activation of JNK1 during ischemia and reperfusion. *J Biol Chem* 1997;**272**:16657–16662.

J Pharmacol Sci **112**, 320 – 326 (2010)

Journal of Pharmacological Sciences

Full Paper

Dictyostelium Differentiation-Inducing Factor-1 Binds to Mitochondrial Malate Dehydrogenase and Inhibits Its Activity

Tomoko Matsuda[1], Fumi Takahashi-Yanaga[1,*], Tatsuya Yoshihara[1], Katsumi Maenaka[2], Yutaka Watanabe[4], Yoshikazu Miwa[1], Sachio Morimoto[1], Yuzuru Kubohara[5], Masato Hirata[3], and Toshiyuki Sasaguri[1]

[1]*Department of Clinical Pharmacology, Faculty of Medical Sciences,* [2]*Medical Institute of Bioregulation,*
[3]*Laboratory of Molecular and Cellular Biochemistry, Faculty of Dental Sciences, Kyushu University, Fukuoka 812-8582, Japan*
[4]*Department of Applied Chemistry, Faculty of Engineering, Ehime University, Matsuyama 790-8577, Japan*
[5]*Biosignal Research Center, Institute for Molecular and Cellular Regulation, Gunma University, Maebashi 371-8512, Japan*

Received December 11, 2009; Accepted January 8, 2010

Abstract. We have reported that the differentiation-inducing factors (DIFs) DIF-1 and DIF-3, morphogens secreted from *Dictyostelium discoideum*, inhibit proliferation of several cancer cells via suppression of the Wnt/β-catenin signaling pathway. However, the target molecules of DIFs involved in the anti-proliferative effects are still unknown. In the present study, DIF-1–tethered resins were synthesized to explore the target molecules of DIFs, and mitochondrial malate dehydrogenase (mMDH) was identified as one of the target molecules. In the in vitro assay, DIF-1 and other analogs including 2-MIDIF-1, DIF-3, and 6-MIDIF-3 were found to be capable of binding to mMDH but not to cytoplasmic MDH. However, only DIF-1 and 2-MIDIF-1 inhibited the enzymatic activity of mMDH. The effects of DIF analogs on ATP content and cell proliferation were then analyzed using HeLa cells. DIF-1 and 2-MIDIF-1 were found to lower the ATP content and both chemicals inhibited HeLa cell proliferation, suggesting that inhibition of mMDH activity affected cell energy production, probably leading to the inhibition of proliferation. These results suggest that the inhibition of mMDH activity by DIF-1 and 2-MIDIF-1 could be one of the mechanisms to induce anti-proliferative effects, independent of the inhibition of the Wnt/β-catenin signaling pathway.

Keywords: differentiation-inducing factor, mitochondrial malate dehydrogenase (mMDH), energy production, ATP content, cell proliferation

Introduction

Differentiation-inducing factors (DIFs), first identified in *Dictyostelium discoideum* as putative morphogens required for stalk cell differentiation (1 – 4), also affect mammalian cells (5 – 8). We reported that DIF-1 and DIF-3 [1-(3,5-dichloro-2,6-dihydroxy-4-methoxyphenyl) hexan-1-one and 1-(3-chloro-2,6-dihydroxy-4-methoxyphenyl)hexan-1-one, respectively] inhibited mammalian cell proliferation by suppressing the Wnt/β-catenin signaling pathway via the activation of glycogen synthase kinase-3β (GSK-3β) (9 – 13). Since the constant activation of the Wnt/β-catenin signaling pathway has frequently been demonstrated in several types of human malignant neoplasms (14, 15), it could be suggested that DIFs are potent antitumor agents and identification of the target molecule(s) for DIFs may offer ideas for the design of new anticancer drugs. However, the target molecule(s) of DIFs involved in the anti-proliferative effect and/or the inhibition of the Wnt/β-catenin signaling pathway are unknown. Shimizu et al. first reported that calmodulin-dependent cyclic nucleotide phosphodiesterase could be a pharmacological target molecule for DIF-1, whereas a specific inhibitor for phosphodiesterase 1 failed to mimic

*Corresponding author. yanaga@clipharm.med.kyushu-u.ac.jp
Published online in J-STAGE on February 20, 2010 (in advance)
doi: 10.1254/jphs.09348FP

the anti-proliferative effect of DIF-1 (16).

In the present study, the target molecules of DIFs were explored. For this purpose, DIF-1–tethered beads for affinity chromatography were synthesized. Upon further investigation, we found that the mitochondrial isoform of malate dehydrogenase (mMDH) was one of the target molecules of DIFs.

Malate dehydrogenase (MDH; EC 1.1.1.37) is an essential enzyme in the tricarboxylic acid cycle and malate-aspartate shuttle (17, 18), oxidizing malate to oxaloacetate and reducing oxaloacetate to malate, respectively. Two isoenzymes of MDH are found in animal tissues: one is in the mitochondria (mMDH, 314 amino acids) and the other is in the cytoplasm (cMDH, 332 amino acids) (19). The major role of mMDH is to oxidize malate to oxaloacetate in the tricarboxylic acid cycle, and that of cMDH is to reduce oxaloacetate to malate in the malate-aspartate shuttle. Since both the tricarboxylic acid cycle and malate-aspartate shuttle play essential roles in the energy production in cells, we analyzed the effect of DIF-1 and other DIF analogs on the activities of MDH in relation to ATP production and cell proliferation using HeLa cells.

Materials and Methods

Materials

DIF-1 and DIF-3 (1-(3,5-dichloro-2,6-dihydroxy-4-methoxyphenyl)hexan-1-one and 1-(3-chloro-2,6-dihydroxy-4-methoxyphenyl)hexan-1-one, respectively) were synthesized according to the procedure of Masento et al. (20). The other DIF analogs (2-MIDIF-1, 2-methoxy isomer of DIF-1, and 6-MIDIF-3, 6-methoxy isomer of DIF-3) were synthesized by Toyama Chemical Co. (Tokyo). Mitochondrial MDH (M2634) and cMDH (M7383) prepared from porcine heart were purchased from Sigma (St. Louis, MO, USA).

Preparation of DIF-1–tethered resin

To a solution of DIF-1 (20 mg, 0.065 mmol) and 2,6-lutidine (11 μL, 0.078 mmol) in CH_2Cl_2 (200 μL) was added 2-chlorethanesulfonyl chloride (8 μL, 0.078 mmol), and the resulting mixture was stirred for 2 h at room temperature. After work-up, silica-gel chromatography (AcOEt/hexane 1:4) gave mono-*O*-ethenesulfonylated DIF-1 (11 mg, 42%) together with DIF-1 (58% recovered). AffiGel 10 (chemical capacity: 0.01 mmol/gel mL; Bio-Rad, Herucles, CA, USA,) was modified by treatment with 2-aminoethanethiol in isopropanol. The modified resin (1 mL) was treated with sulfonyl-DIF-1 (8.0 mg, 0.02 mmol) and triethylamine (3.3 μL, 0.024 mmol) and ethanol (0.5 mL) for 1 h. The resin was obtained by filtration of the mixture and washing with ethanol. It was then similarly treated with *N*-phenylmaleimide (3.5 mg, 0.02 mmol), triethylamine (3.3 μL, 0.024 mmol), and ethanol (0.5 mL) for 3 h in order to cap the residual SH function. After filtration, the DIF-1–tethered affinity resin was obtained.

Cell culture

The human cervical carcinoma cell line HeLa was grown in Dulbecco's modified Eagle's medium (Sigma) supplemented with 10% fetal bovine serum, 100 U/mL penicillin G, and 0.1 mg/mL streptomycin.

Affinity chromatography using DIF-1–tethered resins

Cytoplasmic proteins were prepared from cells cultured in 100-mm dishes using NE-PER™ nuclear and cytoplasmic extraction reagents (Pierce, Rockford, IL, USA). Just before use, 10 μL of DIF-1–tethered-beads were washed with 1 mL of buffer A containing 10 mM Tris-HCl pH 7.4, 1 mM EDTA, 50 mM KCl, and 10% glycerol and then resuspended with 200 μL of the same buffer. The beads were incubated in the presence or absence of 100 μM of DIF-1 at 4°C for 1 h, followed by the addition of the cell extract (1 mg of cytoplasmic proteins) and incubation for an additional 2 h. Proteins bound to the beads were extracted in Laemmli's sample buffer after extensive washing with buffer A.

Identification of binding protein

The extracted protein from the beads was separated by 10% SDS-PAGE, followed by silver staining. The gel pieces with bands only observed in the absence of DIF-1 were treated with trypsin, and the resulting peptides were analyzed by liquid chromatography/mass/mass spectrometry (LC-MS/MS) as described in the previous report (21). Mass spectroscopy data were analyzed by the MASCOT search engine (Matrix Science, Boston, MA, USA) using the International Protein Index (European Bioinformatics Institute, Hinxton, UK) as references.

Quartz crystal microbalance (QCM) assay

To measure the affinity of DIF and its analogs for MDH, a QCM assay was performed as described previously (22) with minor modifications. Briefly, 2 μL of 4 mg/mL mMDH, cMDH or bovine serum albumin (BSA) was fixed on the sensor-tip of the QCM and placed in the chamber filled with 2 mL of phosphate-buffered saline. After the frequency of the sensor-tip was stable, ethanol (vehicle), DIF-1 or the analogs (2 μL; final concentration of 30 μM) were injected into the chamber. The frequency of the chip was measured at 25°C with constant stirring.

Measurement of enzymatic activities of mMDH and cMDH

Activities of mMDH or cMDH were assayed either in

the forward direction (malate + NAD^+ → oxaloacetate + NADH) or reverse direction. Mitochondrial MDH (10.1 mg/mL) or cMDH (7.4 mg/mL) were diluted 1,000-times with a solution containing 0.1 mg/mL BSA and 1 μM dithiothreitol and were pre-incubated with or without DIF-1 (final concentration: 30 μM) for 10 min on ice. Then, 10 μL of the enzyme solution and 40 μL of β-NAD^+ (final concentration: 10 mM) was mixed in a 96-well plate, followed by monitoring at the wavelength of 340 nm using a Flex Station3 micro-plate reader (Molecular Devices, Sunnyvale, CA, USA). Three minutes later, 50 μL of malate (final concentration: 500 mM) was added to the each well as substrate. One unit was defined as the activity that can increase NADH by 1.0 μmol per min.

Intracellular ATP measurement and cell proliferation assay

HeLa cells (2.0×10^4 cells/well) were seeded into 24-well plates and treated with or without 30 μM DIF-1 or the analogs for given periods. Cells were harvested by the trypsin/EDTA treatment and enumerated using a Coulter Counter (Beckman Coulter, Fullerton, CA, USA). Intracellular ATP content was determined with a luciferin–luciferase method using an ATP assay kit (TOYO INK, Tokyo). Luciferase activity was determined with a luminometer (Lumat LB 9507; Berthold Technologies, Bad Wildbad, Germany).

Results

DIF-1 modification and immobilization

Ligand-immobilized beads were used as a tool to identify the target molecules of DIF-1. Therefore, we first synthesized the DIF-1 analog, DIF-1-sulfonate shown in Fig. 1A (see also Fig. 5A for the structure of DIF-1), which could be connected to reactive beads. Assays of cell proliferation was performed using HeLa cells, since we reported that DIF-1 and DIF-3 inhibited mammalian cell proliferation. As shown in Fig. 1B, DIF-1-sulfonate clearly exhibited inhibitory effects on cell proliferation, albeit with a weaker potency than DIF-1, encouraging us to further synthesize DIF-1–tethered beads using the analog.

DIF-1 binds to mMDH and the effects on the enzyme activity

HeLa cell extracts were mixed with immobilized-DIF-1 and affinity chromatography was performed as described in Materials and Methods. To identify the proteins that bind specifically to DIF-1, the cell extracts were incubated with the immobilized beads in the presence or absence of DIF-1 at 4°C for 2 h. Binding proteins were separated by 10% SDS-PAGE and two silver-

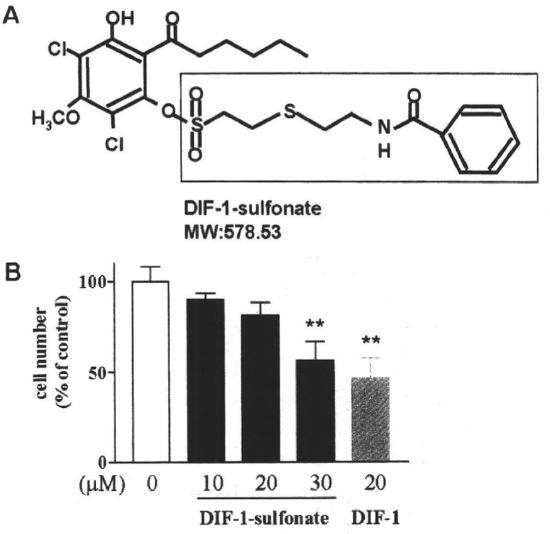

Fig. 1. Chemical structure and effects of DIF-1-sulfonate. A) Structure of DIF-1-sulfonate. The sulfonate group acting as a bridge for connection to the beads is marked by a rectangle. B) Effect of DIF-1-sulfonate on the cell proliferation. HeLa cells were treated with the indicated chemicals for 48 h and enumerated. The reported data are each the mean ± S.D. of three independent experiments (n = 3). $^{**}P < 0.01$ vs. control (by Student's *t*-test).

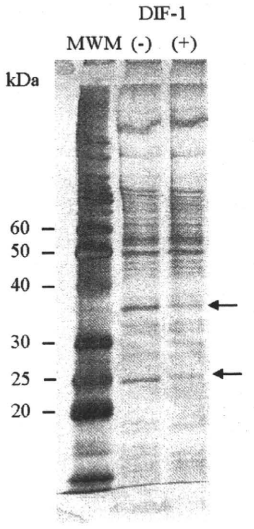

Fig. 2. DIF-1–tethered resin-binding proteins in HeLa cells. The extract from HeLa cells was loaded onto DIF-1–tethered resin with or without excess amount of DIF-1. The bound protein was analyzed by SDS-PAGE followed by silver staining. Arrows indicate two bands that specifically bound to DIF-1–tethered resin.

stained bands were identified as the proteins that bind to DIF-1–tethered beads, but not in the presence of the soluble ligand (Fig. 2). The upper band was identified as mMDH by mass spectrometry, while the lower band was

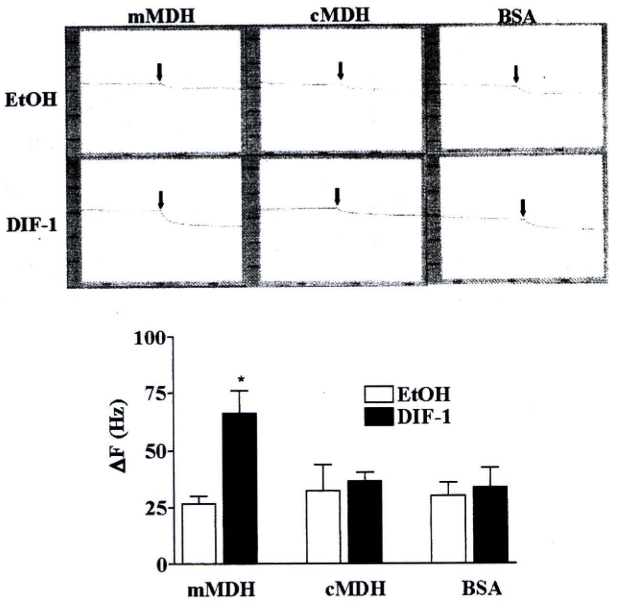

Fig. 3. DIF-1 binds with mMDH. QCM assay was performed as described in Materials and Methods. A difference of frequency was measured before and after injection. The arrows in the upper figure indicate the injection points of vehicle (ethanol: EtOH) or DIF-1. The lower graph shows the difference in frequency between before and after injection. The reported data are each the mean ± S.D. of three independent experiments. $*P < 0.05$ vs. control (by Student's *t*-test).

not identified. To confirm whether DIF-1 binds directly to mMDH in vitro, we performed QCM analysis. As shown in Fig. 3, the frequency was significantly reduced by adding DIF-1 when mMDH was fixed on the sensor tip. No significant changes were observed when cMDH, the cytosolic isoenzyme of MDH or BSA was fixed on the tip, indicating that DIF-1 directly binds to mMDH but not to cMDH. Subsequently, the effect of DIF-1 on the activities of mMDH and cMDH were analyzed. Mitochondrial MDH or cMDH, obtained from a commercial source was assayed for NAD^+-dependent oxidation (forward direction). DIF-1 inhibited mMDH activity in a dose-dependent manner (Fig. 4A), whereas cMDH activity was not affected (Fig. 4B). The result agreed well with the result shown in Fig. 3, indicating that DIF-1 inhibited mMDH activity by direct binding.

Effects of DIF-1 analogs on mMDH

The interactions between mMDH and DIF analogs (2-MIDIF-1, DIF-3, and 6-MIDIF-3) were analyzed by the QCM assay. As shown in Fig. 5A, all DIF analogs examined were revealed to directly bind to mMDH and the positive signals with 2-MIDIF-1 was highest among the analogs examined, suggesting that 2-MIDIF-1 had the highest affinity. The effects of DIF analogs on the enzyme activity were then analyzed (Fig. 5B). Interestingly, of the 3 analogs examined, only 2-MIDIF-1 was inhibitory, although the effect of 2-MIDIF-1 appeared weaker than that of DIF-1 (Figs. 4A and 5B).

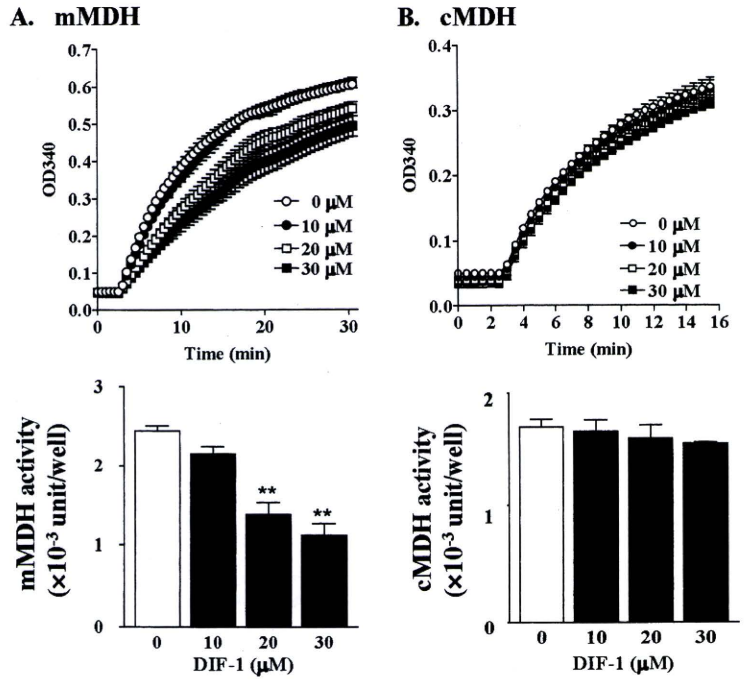

Fig. 4. Effects of DIF-1 on MDH activity. The mMDH (A) and cMDH (B) activities were assayed in the forward direction using different concentrations of DIF-1. Upper panels show the change of absorption and lower panels show the graph for MDH activity calculated from the upper panels as described in Materials and Methods. Each value is the mean ± S.E.M. of three independent experiments done in triplicate. $**P < 0.01$ vs. control (by Student's *t*-test).

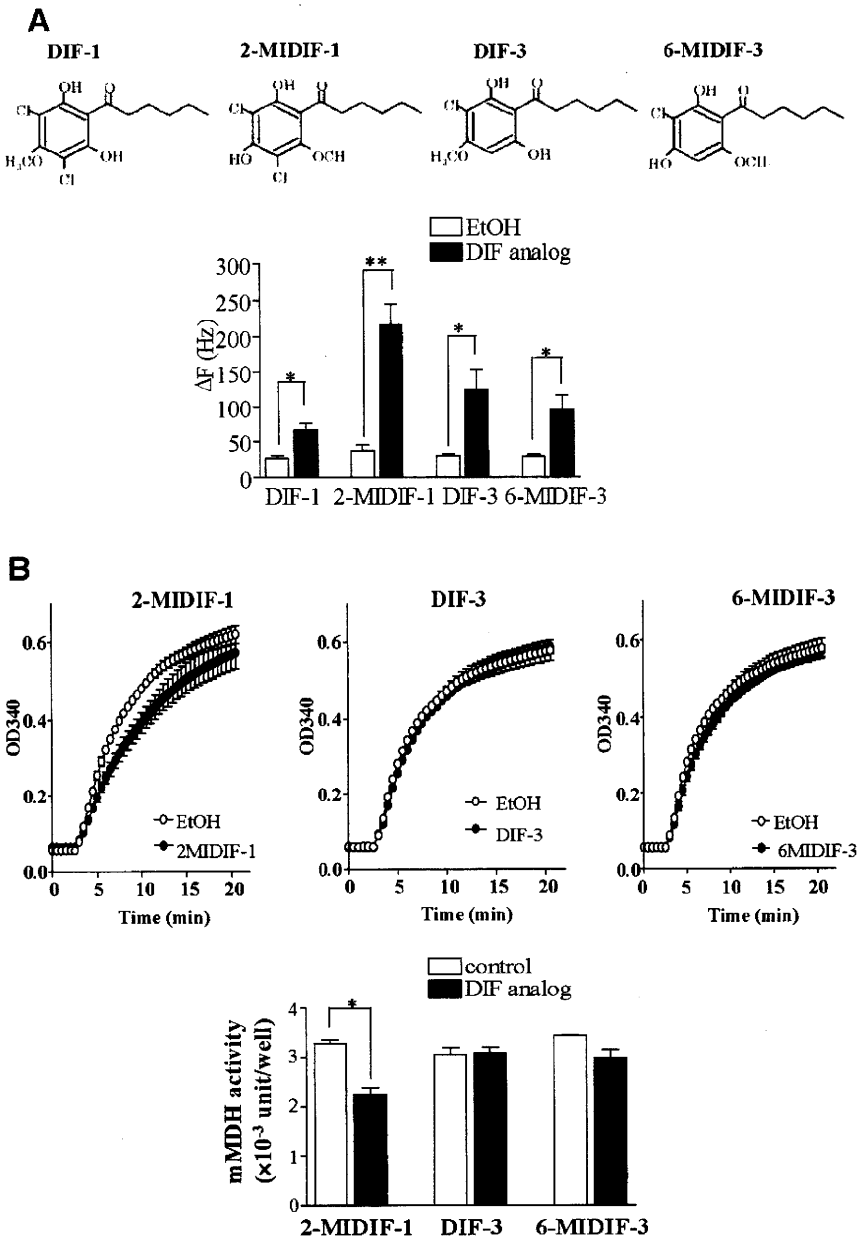

Fig. 5. Effect of DIF analogs on mMDH. A) Upper panel shows the chemical structure of DIF analogs and lower panel shows the binding property of DIF analogs to mMDH. Difference of frequency was measured before and after injection. Data are shown as the difference of frequency between before and after injection. Each value is the mean ± S.E.M of three independent experiments. $*P < 0.05$ vs. control, $**P < 0.01$ vs. control (by Student's *t*-test). B) Effect of DIF analogs on mMDH activity. mMDH activity was measured in the forward direction. Upper panels show the change of absorption and lower panel shows the graph for mMDH activity calculated from the upper panel as described in Materials and Methods. Each value is the mean ± S.E.M. of three independent experiments done in triplicate. $*P < 0.05$ vs. control (by Student's *t*-test).

Effects of DIF-1 and DIF analogs on ATP content and cell growth

To examine the relationship between the inhibition of mMDH activity, cell energy production, and cell proliferation, the effects of DIF analogs on intracellular ATP content and cell proliferation were examined using HeLa cells. The cellular content of ATP was gradually increased as the time of culture increased up to 72 h, and DIF-3 and 6-MIDIF-3, ineffective in the mMDH assay, did not impact the results (Fig. 6A). On the other hand, DIF-1 and 2-MIDIF-1 lowered the ATP content in the same order of potency as that for the inhibition of mMDH activity.

Cell proliferation was also analyzed. As shown in Fig. 6B, DIF-1 and DIF-3 were the most potent inhibitors of the cell proliferation, while 6-MIDIF-3 was ineffective. In the case of 2-MIDIF-1, the inhibition of cell proliferation became evident at 72 h, when the cellular content of ATP was apparently lowered to a similar level as that with DIF-1. However, the ATP content of HeLa cells after 72-h treatment with 2-MIDIF-1 was still approximately 70% of that at time 0, suggesting that 2-MIDIF-

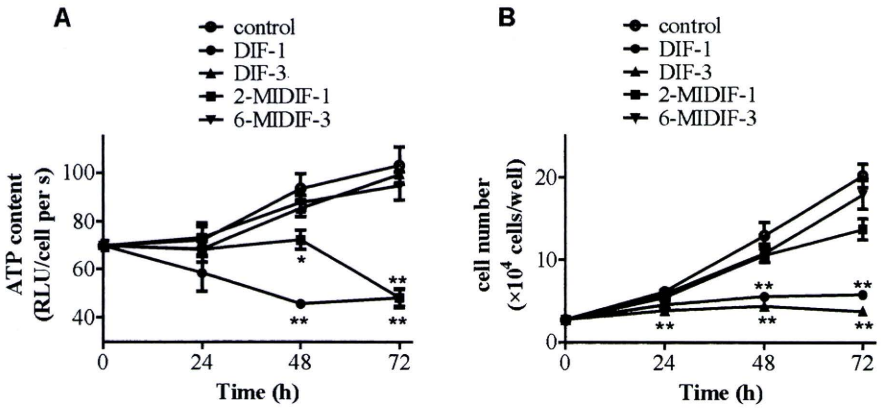

Fig. 6. Effects of DIF analogs on intracellular ATP content and cell growth. HeLa cells (2.0×10^4 cells/well) were seeded into 24-well plates and treated with or without 30 μM of DIF analogs for the given periods. Cells were harvested by trypsin/EDTA treatment, followed by the measurement of the ATP content (A) and cell number (B). The reported data are each the mean ± S.E.M. of three independent experiments, each performed in duplicate. $*P < 0.05$ vs. control, $**P < 0.01$ vs. control (by Student's *t*-test).

1–treated HeLa cells did not deplete ATP. This result was well correlated with the fact that 2-MIDIF-1 showed a weak inhibitory effect on cell proliferation.

Discussion

Previously, we have been reported that DIF-1 and DIF-3 inhibit cell proliferation via the suppression of the Wnt/β-catenin signaling pathway in human cancer cells (9 – 13). Although the purpose of the study was to find the target molecule of DIFs related with the Wnt/β-catenin signaling pathway, unfortunately we could not identify such a protein from mass spectrometry. Mitochondrial MDH, one of the DIFs target proteins found in this study, is not a component of the Wnt/β-catenin signaling pathway and this enzyme was inhibited by only DIF-1 and not by DIF-3, whereas both chemicals showed an inhibitory effect on the Wnt/β-catenin signaling pathway. These observations suggest that other target molecules related with the Wnt/β-catenin signaling pathway must exist. Further studies are required to identify the target molecules of DIF analogs.

We analyzed the changes in cellular content of ATP and cell proliferation in HeLa cells treated with DIF analogs. DIF-1 lowered the ATP content and inhibited cell proliferation more robustly than 2-MIDIF-1. This might have resulted from the fact that DIF-1 exhibited stronger inhibition of mMDH activity than 2-MIDIF-1 and suggest that lowering the ATP content caused by the inhibition of mMDH is pharmacologically relevant to the inhibition of cell proliferation.

Alternatively, a recently reported finding that DIF-1, but not 2-MIDIF-1, was able to promote glucose uptake and consumption could explain the inhibition results (23). It is possible that DIF-1–treated cells deplete glucose in the medium during the culture period. Furthermore, it is well known that glycolysis rather than the tricarboxylic acid cycle is the main energy production system in a number of cancer cell types (24 – 26), suggesting that inhibition of mMDH activity might not have a strong effect on ATP production and inhibition of glycolysis might be more effective to reduce ATP production in HeLa cells. Consequently, depletion of glucose in the culture medium by DIF-1 likely resulted in the decrease of the ATP content in the HeLa cells. This notion also might explain the delay of 2-MIDIF-1 on the ATP content. At the initial stage of the culture, 2-MIDIF-1–treated cells produced ATP mainly using glycolysis, uptaking glucose from the culture medium, but at the later stage, consumption of glucose triggered oxidization of fatty acids to yield acetyl-CoA for the tricarboxylic acid cycle, and gluconeogenesis from amino acids followed by glycolysis, thus producing an overall lower level of ATP.

In this report, we showed that mMDH, one of the essential enzymes in the tricarboxylic acid cycle and malate-aspartate shuttle for main energy production in normal cells, is one of the target molecules of DIFs. Indeed, all DIFs analogs examined in this study could bind to mMDH. However, among the DIF analogs examined, only DIF-1 and 2-MIDIF-1 inhibit mMDH activity, suggesting that the chlorine at the 5 position of the DIF ring is essential for inhibition. Although we have reported that both DIF-1 and DIF-3 inhibited proliferation of human cancer cells, this finding may suggest that DIF-3 is more suitable as a candidate for a new anti-cancer drug than DIF-1, since DIF-3 lacks the chlorine at the 5 position of the DIF ring and does not affect mMDH activity.

Acknowledgments

This work was supported by grants from the Ministry of Education, Culture, Sports, Science and Technology, Japan (a Grant-in-Aid

for Scientific Research). We thank M. Oda and E. Fujimoto in the Laboratory for Technical Support, Medical Institute of Bioregulation, Kyushu University for technical assistance.

References

1 Morris HR, Taylor GW, Masento MS, Jermyn KA, Kay RR. Chemical structure of the morphogen differentiation inducing factor from *Dictyostelium discoideum*. Nature. 1987;328: 811–814.

2 Morris HR, Masento MS, Taylor GW, Jermyn KA, Kay RR. Structure elucidation of two differentiation inducing factors (DIF-2 and DIF-3) from the cellular slime mould *Dictyostelium discoideum*. Biochem J. 1988;249:903–906.

3 Wurster B, Kay RR. New roles for DIF? Effects on early development in *Dictyostelium*. Dev Biol. 1990;140:189–195.

4 Morandini P, Offer J, Traynor D, Nayler O, Neuhaus D, Taylor GW, et al. The proximal pathway of metabolism of the chlorinated signal molecule differentiation-inducing factor-1 (DIF-1) in the cellular slime mould *Dictyostelium*. Biochem J. 1995:306: 735–743.

5 Kubohara Y. DIF-1, Putative morphogen of *D. discoideum*, suppresses cell growth and promotes retinoic acid-induced cell differentiation in HL-60. Biochem Biophys Res Commun. 1997;236: 418–422.

6 Kubohara Y. Effect of differentiation-inducing factors of *Dictyostelium discoideum* on human leukemia K562 cells: DIF-3 is the most potent anti-leukemic agent. Eur J Pharmacol. 1999;381: 57–62.

7 Gokan N, Kikuchi H, Nakamura K, Oshima Y, Hosaka K, Kubohara Y. Structural requirements of *Dictyostelium* differentiation-inducing factors for their stalk-cell-inducing activity in *Dictyostelium* cells and anti-proliferative activity in K562 human leukemic cells. Biochem Pharm. 2005;70:676–685.

8 Miwa Y, Sasaguri T, Kosaka C, Taba Y, Ishida A, Abumiya T, et al. Differentiation-inducing factor-1, a morphogen of dictyostelium, induces G(1) arrest and differentiation of vascular smooth muscle cells. Circ Res. 2000;86:68–75.

9 Takahashi-Yanaga F, Taba Y, Miwa Y, Kubohara Y, Watanabe Y, Hirata M, et al. *Dictyostelium* differentiation-inducing factor-3 activates glycogen synthase kinase-3β and degrades cyclin D1 in mammalian cells. J Biol Chem. 2003; 278:9663–9670.

10 Yasmin T, Takahashi-Yanaga F, Mori J, Miwa Y, Hirata M, Watanabe Y, et al. Differentiation-inducing factor-1 suppresses gene expression of cyclin D1 in tumor cells. Biochem Biophys Res Commun. 2005;338:903–909.

11 Mori J, Takahashi-Yanaga F, Miwa Y, Watanabe Y, Hirata M, Morimoto S, et al. Differentiation-inducing factor-1 induces cyclin D1 degradation through the phosphorylation of Thr^{286} in squamous cell carcinoma. Exp Cell Res. 2005;310:426–433.

12 Takahashi-Yanaga F, Mori J, Matsuzaki E, Watanabe Y, Hirata M, Miwa Y, et al. Involvement of GSK-3β and DYRK1B in differentiation-inducing factor-3-induced phosphorylation of cyclin D1 in HeLa cells. J Biol Chem. 2006;281:38489–38497.

13 Matsuzaki E, Takahashi-Yanaga F, Miwa Y, Hirata M, Watanabe Y, Sato N, et al. Differentiation-inducing factor-1 alters canonical Wnt signaling and suppresses alkaline phosphatase expression in osteoblast-like cell lines. J Bone Miner Res. 2006;21:1307–1316.

14 Barker N, Clevers H. Mining the Wnt pathway for cancer therapeutics. Nat Rev Drug Discov. 2006;5:997–1014.

15 Fodde R, Brabletz T. Wnt/β-catenin signaling in cancer stemness and malignant behavior. Curr Opin Cell Biol. 2007;19:150–158.

16 Shimizu K, Murata T, Tagawa T, Takahashi K, Ishikawa R, Abe Y, et al. Calmodulin-dependent cyclic nucleotide phosphatase (PDE1) is a pharmacological target of differentiation-inducing factor-1, an antitumor agent isolated from Dictyostelium. Cancer Res. 2004;64:2568–2571.

17 Goward CR, Nicholls DJ. Malate dehydrogenase: a model for structure, evolution, and catalysis. Protein Sci. 1994;3:1883–1888.

18 LaNoue KF, Bryla J, Bassett DJ. Energy-driven aspartate efflux from heart and liver mitochondria. J Biol Chem. 1974;249:7514–7521.

19 Joh T, Takeshima H, Tsuzuk T, Setoyama C, Shimada K, Tanase S, et al. Cloning and sequence analysis of cDNAs encoding mammalian cytosolic malate dehydrogenase. Comparison of the amino acid sequences of mammalian and bacterial malate dehydrogenase. J Biol Chem. 1987;262:15127–15131.

20 Masento MS, Morris HR, Taylor G, Johnson SJ, Skapski AC, Kay RR. Differentiation-inducing factor from the slime mould Dictyostelium discoideum and its analogues. Synthesis, structure and biological activity. Biochem J. 1988;256:23–28.

21 Matsumoto M, Hatakeyama S, Oyamada K, Oda Y, Nishimura T, Nakayama KI. Large-scale analysis of the human ubiquitin-related proteome. Proteomics. 2005;5:4145–4151.

22 Lu Q-W, Morimoto S, Harada K, Du C-K, Takahashi-Yanaga F, Miwa Y, et al. Cardiac troponin T mutation R141W found in dilated cardiomyopathy stabilizes the troponin T-tropomyosin interaction and causes Ca2+ deswnsitization. J Mol Cell Cardiol. 2003;35:1421–1427.

23 Omata W, Shibata H, Nagasawa M, Kojima I, Kikuchi H, Oshima Y, et al. Dictyostelium differentiation-inducing factor-1 induces glucose transporter 1 translocation and promotes glucose uptake in mammalian cells. FEBS J. 2007;274:3392–3404.

24 Warburg O. On the origin of cancer cells. Science. 1956;123: 309–314.

25 Shaw RJ. Glucose metabolism and cancer. Curr Opin Cell Biol. 2006;18:598–608.

26 Ganapathy V, Thangaraju M, Prasad PD. Nutrient transporters in cancer: relevance to Warburg hypothesis and beyond. Pharmacol Ther. 2009;121:29–40.

BJP BRITISH JOURNAL OF PHARMACOLOGY
BPS BRITISH PHARMACOLOGICAL SOCIETY

BJP British Journal of Pharmacology

DOI:10.1111/j.1476-5381.2010.00942.x
www.brjpharmacol.org

RESEARCH PAPER

Biological actions of green tea catechins on cardiac troponin C

Naoto Tadano[1,2*]; Cheng-Kun Du[1*], Fumiaki Yumoto[3,4*], Sachio Morimoto[1], Mika Ohta[1], Ming-Fang Xie[1], Koji Nagata[3], Dong-Yun Zhan[1], Qun-Wei Lu[1], Yoshikazu Miwa[1], Fumi Takahashi-Yanaga[1], Masaru Tanokura[3], Iwao Ohtsuki[4] and Toshiyuki Sasaguri[1]

[1]*Department of Clinical Pharmacology, Graduate School of Medical Sciences, Kyushu University, Fukuoka, Japan,* [2]*Research Laboratory, Zenyaku Kogyo Co., Ltd, Tokyo, Japan,* [3]*Deprartment of Applied Biological Chemistry, Graduate School of Agricultural and Life Sciences, University of Tokyo, Tokyo, Japan, and* [4]*Department of Physiology, The Jikei University School of Medicine, Tokyo, Japan*

Correspondence
Sachio Morimoto, Department of Clinical Pharmacology, Graduate School of Medical Sciences, Kyushu University, Fukuoka 812-8582, Japan. E-mail: morimoto@med.kyushu-u.ac.jp

*These authors contributed equally to this work.

Keywords
catechin; gallate; troponin; calcium sensitivity; cardiomyopathy

Received
25 March 2010
Revised
19 May 2010
Accepted
6 June 2010

BACKGROUND AND PURPOSE

Catechins, biologically active polyphenols in green tea, are known to have a protective effect against cardiovascular diseases. In this study, we investigated direct actions of green tea catechins on cardiac muscle function to explore their uses as potential drugs for cardiac muscle disease.

EXPERIMENTAL APPROACH

The effects of catechins were systematically investigated on the force-pCa relationship in skinned cardiac muscle fibres to determine their direct effects on cardiac myofilament contractility. The mechanisms of action of effective catechins were investigated using troponin exchange techniques, quartz crystal microbalance, nuclear magnetic resonance and a transgenic mouse model.

KEY RESULTS

(-)-Epicatechin-3-gallate (ECg) and (-)-epigallocatechin-3-gallate (EGCg), but not their stereoismers (-)-catechin-3-gallate and (-)-gallocatechin-3-gallate, decreased cardiac myofilament Ca^{2+} sensitivity probably through its interaction with cardiac troponin C. EGCg restored cardiac output in isolated working hearts by improving diastolic dysfunction caused by increased myofilament Ca^{2+} sensitivity in a mouse model of hypertrophic cardiomyopathy.

CONCLUSIONS AND IMPLICATIONS

The green tea catechins, ECg and EGCg, are Ca^{2+} desensitizers acting through binding to cardiac troponin C. These compounds might be useful compounds for the development of therapeutic agents to treat the hypertrophic cardiomyopathy caused by increased Ca^{2+} sensitivity of cardiac myofilaments.

Abbreviations

cTn, cardiac muscle troponin; EC, (-)-Epicatechin; ECg, (-)-Epicatechin-3-gallate; EGC, (-)-Epigallocatechin; EGCg, (-)-Epigallocatechin-3-gallate; fsTn, fast skeletal muscle troponin; HCM, hypertrophic cardiomyopathy; QCM, quartz crystal microbalance; Tn, troponin

Introduction

A number of studies suggest that consumption of green tea decreased the risk of several pathological conditions, including cardiovascular disease (Wang *et al.*, 1995; Arts *et al.*, 2001; Mukamal *et al.*, 2002). Green tea contains catechins as biologically active polyphenols. Major catechins in green tea are (-)-epicatechin (EC), (-)-epigallocatechin (EGC), (-)-epicatechin-3-gallate (ECg), and

(-)-epigallocatechin-3-gallate (EGCg). ECg and EGCg have been shown to be effective against cardiovascular and other diseases (Chyu *et al.*, 2004; Tachibana *et al.*, 2004; Sasazuki *et al.*, 2008). Mechanisms involved in the prevention of cardiovascular diseases by EGCg have so far been suggested to be associated with its anti-oxidative effect (Chyu *et al.*, 2004), anti-inflammatory effect (Ludwig *et al.*, 2004) and vasorelaxant effect (Lorenz *et al.*, 2004) on the cardiovascular system.

In the present study, we systematically investigated the effects of catechins on the force-pCa relationship in membrane-permeabilized (skinned) cardiac muscle fibres and found that ECg and EGCg have Ca^{2+}-desensitizing effects on the muscle contraction (i.e. effects of decreasing the myofilament Ca^{2+} sensitivity). Hypertrophic cardiomyopathy (HCM) is a cardiac muscle disease characterized by a reduced diastolic function leading to heart failure. Recent genetic investigations revealed that a majority of HCM is caused by mutations in genes for sarcomeric proteins, and increased myofilament Ca^{2+} sensitivity was demonstrated to be a primary functional defect triggering the pathogenesis of HCM (Harada and Morimoto, 2004; Ahmad *et al.*, 2005; Morimoto, 2008; Morimoto, 2009). Although cardioprotective agents such as β-blockers or Ca^{2+} antagonists have been used in the treatment of HCM, there is no reliable evidence that these drugs protect patients with HCM from sudden death and no effective pharmacotherapy is established at present. In this study, we examined the effect of EGCg on the cardiac haemodynamics in a mouse model of HCM, caused by a troponin (Tn) mutation. The results suggest that the green tea catechins might be useful for the development of therapeutic agents to treat the HCM associated with an increased cardiac myofilament Ca^{2+} sensitivity. Part of this work has been reported previously in abstract form (Tadano *et al.*, 2005a,b).

Methods

Animals

All animal care in this investigation conformed to the *Guide for the Care and Use of Laboratory Animals* published by the US National Institutes of Health (NIH Publication no. 85–23, revised 1996). The experimental protocol was reviewed by the Committee of Ethics on Animal Experiments at the Faculty of Medicine, Kyushu University, and carried out according to the *Guidelines for Animal Experiments*, Faculty of Medicine, Kyushu University, and The Law (No. 105) and Notification (No. 6) of the Japanese Government.

Skinned muscle preparation and whole Tn exchange in skinned muscle fibres

Skinned muscle fibres were prepared from the left ventricular trabeculae and the back muscle of young male albino rabbits (2–2.5 kg) as described previously (Morimoto *et al.*, 1998). Endogenous Tn in cardiac and fast skeletal muscle skinned muscle fibres were exchanged with whole rabbit fast skeletal muscle Tn (fsTn) and cardiac muscle Tn (cTn), respectively, as described previously (Mirza *et al.*, 2005). After force measurements, fibre samples were analysed by a 5–20% gradient SDS-PAGE, stained with silver, and the extent of Tn exchange was determined by an optical densitometric scan of the gel (Morimoto *et al.*, 2002).

Preparation of cTn subunits

Human cTn subunits, cTnT, cTnI and cTnC, were expressed in *Escherichia coli* strain BL21(DE3)-CodonPlus-RP (Stratagene, La Jolla, CA, USA) using the expression vector pET-3a (EMD Biosciences, Madison, WI, USA). cTnC was purified with DEAE-Toyopearl 650M (Tosoh, Tokyo, Japan) and an FPLC gel filtration column, Superdex75 26/60 (GE Healthcare Bio-Sciences Corp, Piscataway, NJ, USA). cTnT was purified with DEAE-Toyopearl 650 M (Tosoh) and CM-Toyopearl 650M (Tosoh) in the presence of 6 M urea. cTnIs were purified with CM-Toyopearl 650M (Tosoh) and an FPLC ion-exchange column, MonoS (GE Healthcare) in the presence of urea. After removing urea by dialysis, cTnT and cTnI were used for the experiments.

EGCg binding to cTn subunits

Binding of EGCg to cTnT, cTnI and cTnC were measured using a 27 MHz quartz crystal microbalance (QCM, Initium, Inc., Tokyo, Japan), which is a very sensitive mass measuring apparatus (Okahata *et al.*, 1998a,b; Lu *et al.*, 2003), Biotinylated cTnT, cTnI or cTnC was immobilized on the avidin-coated QCM Au electrode and the sensor tips were immersed in a solution consisting of (in mM) 50 MOPS/KOH (pH 7.0), 300 KCl, 1 $MgCl_2$ and 4 EGTA: high ionic strength conditions were adopted to prevent cTnT and cTnI from being in abnormal conformations. The bindings of EGCg to cTnT, cTnI and cTnC were detected from the frequency changes (ΔF) due to changes in mass on the electrode at sub-nanogram levels upon cumulative injection of EGCg into the bathing solution.

Binding of cTnI N-terminal peptide to cTnC

A synthetic peptide for the N-terminal helix region of cTnI (AKKKSKISASRKLQLKTLLLQIAKQELE) was purchased from Greiner Bio-One (Tokyo, Japan).